Transient response of piezoelectric composites caused by the sudden formation of localized defects

Jacob Aboudi *

Faculty of Engineering, Tel Aviv University, Ramat Aviv 69978, Israel

ARTICLE INFO

ABSTRACT

A continuum model is presented which is capable of generating the transient electroelastic field in piezoelectric composites of periodic microstructure, caused by the sudden appearance of localized defects. These defects are simulated by associating to every one of the ten piezoelectric parameters of the constituents a distinct damage variable. This procedure enables the modeling of localized cracks, soft and stiff inclusions and cavities. As a result, the constitutive equations of the piezoelectric phases appear in a specific form that includes eigen-electromechanical field variables which represent these defects. The method of solution is based on the combination of two distinct approach. In the first one, the representative cell method is employed according to which the periodic composite, which is discretized into several cells, is reduced to a problem of a single cell in the discrete Fourier transform domain. The resulting coupled elastodynamic and electric equations, initial, boundary and interfacial conditions in the transform domain are solved by employing a wave propagation in piezoelectric composite analysis which forms the second approach. The method of solution is verified by comparison with an analytical solution for the transient response of a piezoelectric material with a semi-infinite mode III-crack. Several applications are presented for the sudden formation of cracks in homogeneous and layered piezoelectric materials which are subjected to various types of electromechanical loading, and for the sudden appearance of a cavity. The effect of electromechanical coupling on the dynamic response is discussed.

© 2013 Elsevier Ltd. All rights reserved.

1. Introduction

The utilization of elastic waves to detect crack-like and notch-like defects and flaws is a well known tool in a non-destructive approach for the evaluation and monitoring the integrity of composites and structures, see Rose (1999), Achenbach (2000) and Rizzo and Lanza (2007), for a monograph and two reviews. A quantitative understanding of the response of a solid body with defects to the sudden application of a signal (e.g., the scattering of elastic waves by cracks, inclusions and cavities) requires the solution of an appropriate initial-boundary value transient elastic problem. Similarly, the non-destructive evalution of layered and composite materials by monitoring their dynamic response requires the establishment of elastic wave propagation solutions in such materials. Thus, Saravanos and Hopkins (1996) identified the effect of delaminations by monitoring wave damping. Consequently, and as it has been mentioned by Achenbach (2000), solutions to elastodynamic problems form a basic tool for the quantitative non-destructive monitoring, testing and damage detectors.

Due to the existence of coupling between elastic and electric field, piezoelectric materials form an important class of smart materials which can be utilized for detection, actuation and sensing. They can be used as adapting elements for the monitoring of a structure by providing a response to externally applied conditions, see Rao and Sunar (1994) for a survey. Some piezoelectric materials are brittle (e.g., lead zirconate titanate (PZT) is a very stiff and brittle piezoelectric material). Hence fracture may take place during fabrication and service. Several types of flaws in multilayer actuators have been described by Winzer et al. (1989). Piezoelectric materials have been also employed for the non-destructive monitoring and detection of delamination in composite structures by attaching to them to the structure or embedding them within, see Saravanos et al. (1994), Chee et al. (1998) and Tan and Tong (2007), for example. Thus, just like elastodynamic problems, solutions of dynamic piezoelectric problems should be important in the non-destructive monitoring and testing when such materials are employed. Extensive discussions of various types of damage in composite materials can be found in Talreja and Singh (2012).

* Tel.: +972 3 6408131; fax: +972 3 6407617.
  E-mail address: aboudi@eng.tau.ac.il

In a recent investigation, (Aboudi, 2013a), a method has been presented for the prediction of the elastodynamic stress field in periodically layered composite in which localized defects in the form of a crack, inclusion, cavity or H-crack (transverse crack in a layer together with two interfacial cracks between the adjacent layers) exist. Due to the existence of these types of localized damage, the periodicity of the composite is lost and it is not possible anymore to analyze a repeating unit cell which represents the entire composite since such a representative identity does not exist. The method of solution was based on the combination of two distinct approach. In the first one, the representative cell method (which in the static case was formulated by Ryvkin and Nuller (1997)) was employed according to which the periodic composite with its localized defects is discretized into several cells, and subsequently reduced to a problem of a *single* cell in the discrete Fourier transform domain which is a significant advantage. The resulting elastodynamic equations, initial, boundary and interfacial conditions in the transform domain were solved by employing a wave propagation in composite analysis (originally formulated by Aboudi (1987)) which forms the second approach. The accuracy and reliability of this method of solution was verified by comparisons with five different cases where either analytical solutions are available or a different method of analysis is used.

There are several investigations which concern with the analysis of harmonic waves in piezoelectric composites (e.g., Nayfeh et al. (1999a) and Nayfeh et al. (1999b)), and piezoelectric/piezomagnetic composites (e.g., Chen et al. (2007), Pang et al. (2008) and Du et al. (2009)). Analyses of the transient response of piezoelectric composites are frequently conducted by employing a finite element procedure, see Wang et al. (2011) and references cited there.

The present investigation forms a contribution to the study of the response to dynamic electromechanical loadings of piezoelectric composites with localized defects. It is based on generalizing the aforementioned elastodynamic analysis of Aboudi (2013a) to incorporate the electrical effects. This is performed by coupling the elastodynamic analysis to the presently derived one which considers the electrical field and its dependence on the mechanical deformations. Since the former analysis has been already presented in Aboudi (2013a), only the latter is discussed here and its details are given in the Appendix. As in Aboudi (2013a), the localized defects are modeled by introducing damage variables everyone of which is associated with a piezoelectric material parameter of the constituents. As a result, the piezoelectric constitutive equations are formulated by the inclusion of terms which involve these damage variables and subsequently representing these terms as eigen-electromechanical field. This approach has been successfully implemented by Aboudi (2013b) in static piezoelectric/piezomagnetic deformation problems where it has been shown that it enables the modeling of cracks, stiff and soft inclusions as well as cavities and H-cracks. The accuracy of the present coupled generalization is verified by comparisons with the analytical solution of Li (2001) for the transient response of a piezoelectric material with a semi-infinite mode-III crack.

This article is organized as follows. It begins by formulating the governing and constitutive equations, followed by the method of solution where the representative cell method and wave propagation in piezoelectric composites are presented. The solution strategy discusses the procedure for the coupling between the elastodynamic and the electric analyses. The verification of the method is presented in Section 4 which follows by various applications on the sudden formation of defects in the form of cracks and cavities. The article is concluded by discussing possible generalizations of the proposed approach.

2. Governing equations

Consider a piezoelectric composite which is initially subjected to a system of stresses $\boldsymbol{\sigma}^0$ and electrical displacements $\boldsymbol{D}^0$. It is assumed that at time $t = 0$ defects of certain configurations suddenly appear. Fig. 1(a) shows, for example, a periodically layered piezoelectric composites in which every layer is a piezoelectric material. The defect may represent a crack, a notch, a cavity or an inclusion. This figure shows that the defect appears in one of the layers. In the absence of the defect a periodically layered piezoelectric composite is obtained. Its effective piezoelectric properties can be determined by a suitable micromechanical model such as the high-fidelity generalized of cells (HFGMC) method, (Aboudi et al., 2013).

In the absence of body forces, the fully coupled wave equations in a piezoelectric material are given, (Auld, 1973), by the dynamic equations

$$\nabla \cdot \boldsymbol{\sigma} = \rho \frac{\partial^2 \boldsymbol{u}}{\partial t^2} \tag{1}$$

where $\boldsymbol{u}, \boldsymbol{\sigma}, \rho$ and t denote the mechanical displacement vector, stress tensor, material density and time, respectively. The constitutive relations of the piezoelectric material in which the poling (axis of symmetry) is oriented in the x_3-direction are given by

$$\begin{Bmatrix} \sigma_{11} \\ \sigma_{22} \\ \sigma_{33} \\ \sigma_{23} \\ \sigma_{13} \\ \sigma_{12} \end{Bmatrix} = \begin{bmatrix} c_{11} & c_{12} & c_{13} & 0 & 0 & 0 \\ & c_{11} & c_{13} & 0 & 0 & 0 \\ & & c_{33} & 0 & 0 & 0 \\ & & & c_{44} & 0 & 0 \\ & & & & c_{44} & 0 \\ \text{sym.} & & & & & \frac{1}{2}(c_{11}-c_{12}) \end{bmatrix} \begin{Bmatrix} \epsilon_{11} \\ \epsilon_{22} \\ \epsilon_{33} \\ 2\epsilon_{23} \\ 2\epsilon_{13} \\ 2\epsilon_{12} \end{Bmatrix} - \begin{bmatrix} 0 & 0 & e_{31} \\ 0 & 0 & e_{31} \\ 0 & 0 & e_{33} \\ 0 & e_{15} & 0 \\ e_{15} & 0 & 0 \\ 0 & 0 & 0 \end{bmatrix} \begin{Bmatrix} E_1 \\ E_2 \\ E_3 \end{Bmatrix} \tag{2}$$

In these equations, ϵ_{rs} denotes the elements of the mechanical strain tensor, E_r are the components of the electrical field, the terms c_{rs} represent the components of the elastic stiffnesses and e_{rs} are the elements of the piezoelectric tensor, The components of the small strain tensor ϵ_{rs} are expressed in terms of the displacement components u_r by

$$\epsilon_{rs} = \frac{1}{2}\left(\frac{\partial u_r}{\partial x_s} + \frac{\partial u_s}{\partial x_r}\right) \quad r,s = 1,2,3 \tag{3}$$

The other governing equations are given by

$$-\nabla \times \nabla \times \boldsymbol{E} = \mu_0 \left(\boldsymbol{\kappa} \frac{\partial^2 \boldsymbol{E}}{\partial t^2} + \boldsymbol{e} \nabla_s \frac{\partial^2 \boldsymbol{u}}{\partial t^2} \right) \tag{4}$$

where μ_0 and $\boldsymbol{\kappa}$, are magnetic permeability constant in vacuum and the dielectric tensor, respectively. In Eq. (4), ∇_s indicates that this operator takes the symmetric part.

A great simplification can be achieved by adopting the quasi-static approximation (Auld, 1973; Parton and Kudryavtsev, 1988) which is based on the fact that the elastic waves are about five orders of magnitude slower than the electromagnetic waves. It follows that the magnetic effects caused by the elastic field can be neglected. As a result, $\nabla \times \boldsymbol{E} = \boldsymbol{0}$ which follows from Maxwell equation, and an electric potential ψ can be introduced such that

$$\boldsymbol{E} = -\nabla \psi \tag{5}$$

Hence, Eq. (4) can be replaced by

$$\nabla \cdot \boldsymbol{D} = 0 \tag{6}$$

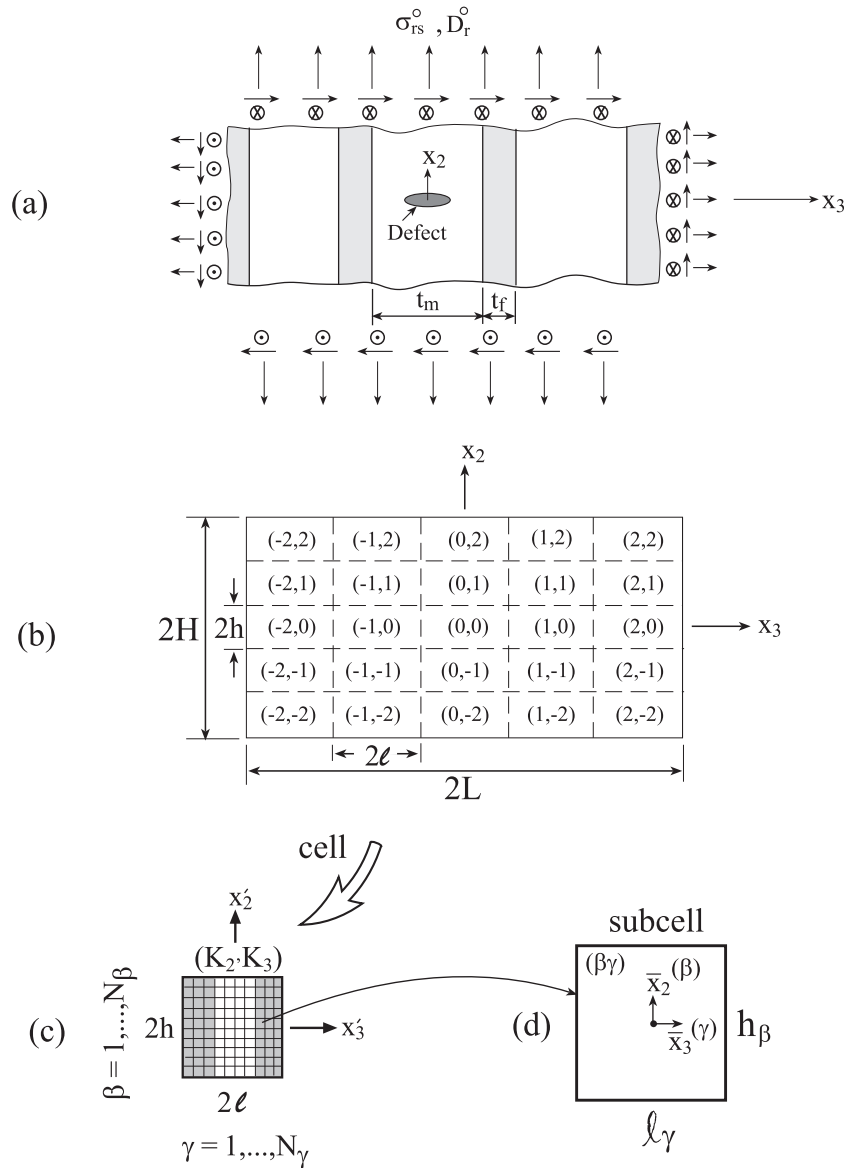where $\boldsymbol{D}$ is the electric displacement which is given by

Fig. 1. (a) A composite which consists of two periodic piezoelectric layers with a localized defect. The periodically layered composite is initially subjected to a system of stresses σ_{rs}^0 and electrical displacements D_r^0. (b) A region $2H \times 2L$ of the composite is divided by repeating cells labeled by (K_2, K_3), the size of every one of which is $2h \times 2l$. (c) A characteristic cell (K_2, K_3) in which local coordinates (x_2', x_3') are introduced. This cell which comprises the two piezoelectric materials is discretized into $N_\beta \times N_\gamma$ subcells. (d) A typical subcell $(\beta\gamma)$ in which a local system of coordinates $(\bar{x}_2^{(\beta)}, \bar{x}_3^{(\gamma)})$ is introduced the origin of which is located at the center. The size of the subcell is $h_\beta \times l_\gamma$.

$$\begin{Bmatrix} D_1 \\ D_2 \\ D_3 \end{Bmatrix} = \begin{bmatrix} 0 & 0 & 0 & 0 & e_{15} & 0 \\ 0 & 0 & 0 & e_{15} & 0 & 0 \\ e_{31} & e_{31} & e_{33} & 0 & 0 & 0 \end{bmatrix} \begin{Bmatrix} \epsilon_{11} \\ \epsilon_{22} \\ \epsilon_{33} \\ 2\epsilon_{23} \\ 2\epsilon_{13} \\ 2\epsilon_{12} \end{Bmatrix} + \begin{bmatrix} \kappa_{11} & 0 & 0 \\ 0 & \kappa_{11} & 0 \\ 0 & 0 & \kappa_{33} \end{bmatrix} \begin{Bmatrix} E_1 \\ E_2 \\ E_3 \end{Bmatrix} \quad (7)$$

It can be readily observed that for a monolithic material, there are five independent stiffnesses c_{ij}, three independent piezoelectric e_{ij} parameters and two dielectric κ_{ij} constants.

Let us also define the vectors **X** and **Y** as follows:

$$\mathbf{X} = [\epsilon_{11}, \epsilon_{22}, \epsilon_{33}, 2\epsilon_{23}, 2\epsilon_{13}, 2\epsilon_{12}, -E_1, -E_2, -E_3] \quad (8)$$

$$\mathbf{Y} = [\sigma_{11}, \sigma_{22}, \sigma_{33}, \sigma_{23}, \sigma_{13}, \sigma_{12}, D_1, D_2, D_3] \quad (9)$$

Consequently, Eqs. (2) and (7) can be written in the following compact matrix form:

$$\mathbf{Y} = \mathbf{Z} : \mathbf{X} \quad (10)$$

where the square 9th-order symmetric matrix of coefficients **Z** has the following form

$$\mathbf{Z} = \begin{bmatrix} \mathbf{C} & \mathbf{e}^T \\ \mathbf{e} & -\boldsymbol{\kappa} \end{bmatrix} \quad (11)$$

In Eq. (11), **C** is the 6th-order stiffness matrix, $\mathbf{e}^T$ denotes the transpose of the rectangular 3 by 6 piezoelectric matrix and $\boldsymbol{\kappa}$ is the square dielectric matrix of order 3. Finally, initial and boundary conditions should be included to complete the formulation of the problem of wave propagation in piezoelectric materials

In order to include the effects of localized defects in the considered piezoelectric materials, 10 independent damage variables $0 \leqslant d_{pq} \leqslant 1, p, q = 1, \ldots, 9$, are associated with every one of the 10 independent elements of Z_{pq} (since for a monolithic material

Table 1
Material density and elastic properties.

Material	$\rho(\text{kg/m}^3)$	$C_{11}(\text{GPa})$	$C_{12}(\text{GPa})$	$C_{13}(\text{GPa})$	$C_{33}(\text{GPa})$	$C_{44}(\text{GPa})$
BaTiO$_3$	5700	166	77	78	162	43
Cadmium Selenide	5820	74.1	45.2	39.3	83.6	13.2

Table 2
Electric properties.

Material	$e_{15}(\text{C/m}^2)$	$e_{31}(\text{C/m}^2)$	$e_{33}(\text{C/m}^2)$	$\kappa_{11}(10^{-12}\text{ C/Vm})$	$\kappa_{33}(10^{-12}\text{ C/Vm})$
BaTiO$_3$	11.6	−4.4	18.6	11,200	12,600
Cadmium Selenide	0.138	−0.16	0.347	82.6	90.3

there are 10 independent constants and therefore, there are 10 corresponding independent damage variables). Thus, Eq. (10) takes the form

$$Y_r = \sum_{s=1}^{9} Z_{rs}(1 - d_{rs})X_s, \quad r = 1, \dots, 9 \tag{12}$$

As in Aboudi (2013a) and Aboudi (2013b), let us write this equation in the form

$$\boldsymbol{Y} = \boldsymbol{Z} : \boldsymbol{X} - \boldsymbol{Y}^{e} \tag{13}$$

where of $\boldsymbol{Y}^{e}$ can be considered as electro-elastic eigen-field vector whose components are given by

$$Y_r^e = \sum_{s=1}^{9} Z_{rs}d_{rs}X_s, \quad r = 1, \dots, 9 \tag{14}$$

As has been shown in Aboudi (2013b), a proper selection of the 10 independent damage variables d_{rs} enables the modeling of localized defects in the form of cracks, notches, stiff and soft inclusions and cavities embedded in the material. For elastic isotropic materials just two independent damage variables would be needed, c.f. Ju (1990).
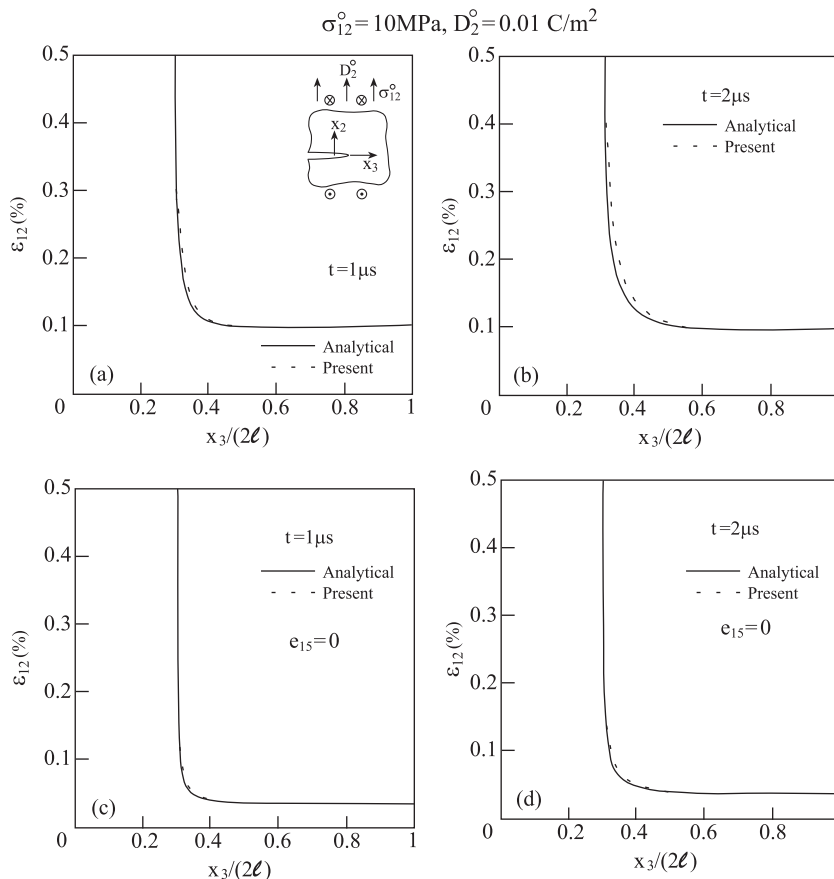

Fig. 2. Comparisons between the analytical and present solutions along the crack's line caused by the sudden appearance of a semi-infinite crack $x_3 \leqslant 0.3$ embedded in a piezoelectric Cadmium Selenide material (poling in the x_1-direction) that is initially subjected to axial shear mechanical loading $\sigma_{12} = 10$ MPa and electric displacement $D_2 = 0.01$ C/m^2. (a) $t = 1$ μs, (b) $t = 2$ μs. (c) and (d) The corresponding comparisons in the absence of electromechanical coupling ($e_{15} = 0$).
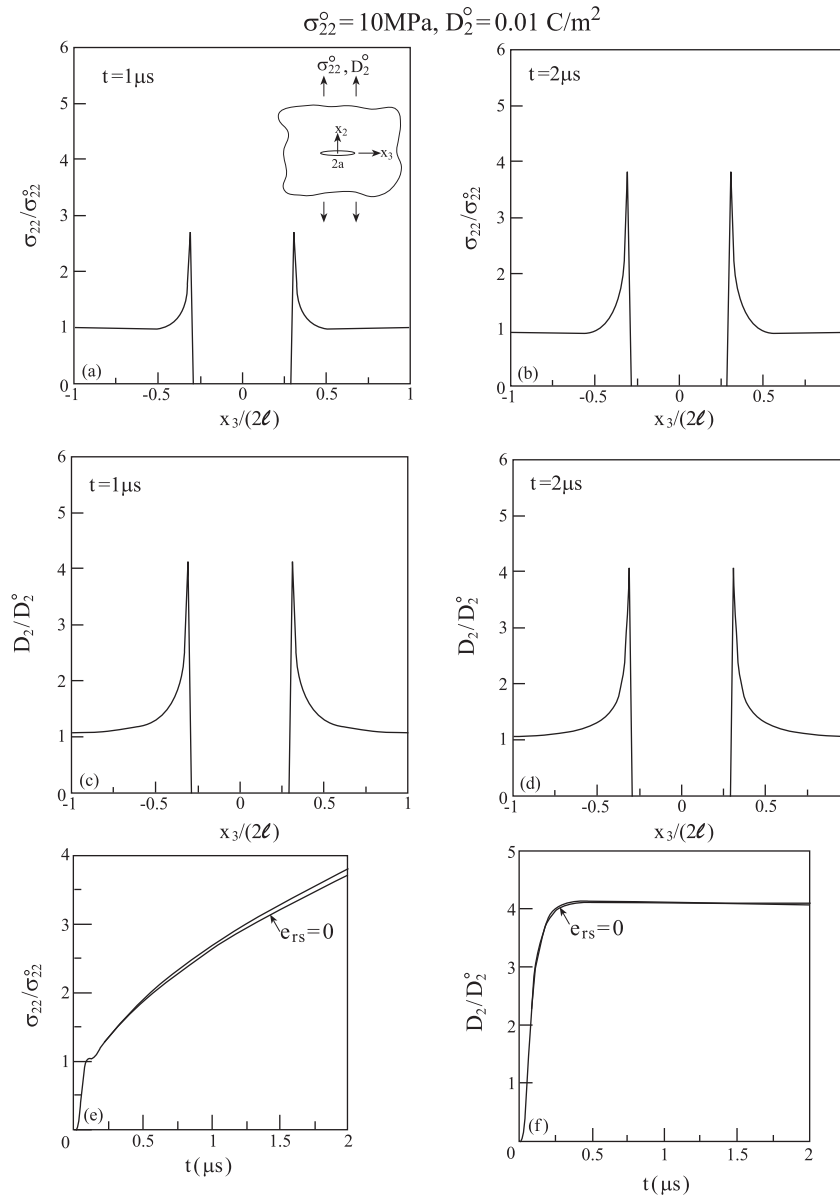
Fig. 3. The variations of the normal stress and electric displacement along the crack line caused by the sudden appearance of of a crack $-0.3 \leqslant x_3/(2l) \leqslant 0.3$ caused by the application of initial field $\sigma_{22}^0 = 10 MPa, D_2^0 = 0.01$ C/m^2 in piezoelectric Cadmium Selenide material. (a) and (b) Normal stress variations, (c) and (d) electric displacement variations. (e) and (f) The time variations of the normal stress and electric displacement at the closest point ahead of the tip in the coupled and uncoupled cases.

For cracks, notches and cavities, the 5 independent elements $c_{11}, c_{12}, c_{13}, c_{33}, c_{44}$ in Eq. (2), as well as the 3 constants e_{31}, e_{33}, e_{15}, and the 2 coefficients κ_{11}, κ_{33} in Eq. (7) are set to be zero. Hence we set $d_{rs} = 1$ for the damage variables which correspond to these 10 independent elements. Therefore the introduction of the damage variables d_{rs} in Eq. 13,14 forms a mean to deteriorate the values of these 10 elements to zero for the modeling of a region that is occupied by a crack, notch or cavity.

3. Method of solution

The method of solution of the problems described above is based on the combination of the representative cell method which was originally presented by Ryvkin and Nuller (1997) in the elastostatic case, and the analysis of wave propagation in elastic composites, (Aboudi et al., 2013). The latter has been recently extended by Aboudi (2013a) to accommodate the initial stresses and the eigen-stresses. Presently, this theory needs to be further

generalized to incorporate the coupled electrical effects of the piezoelectric constituents.

3.1. The representative cell method

According to the representative cell method (not to be confused with the representative volume element (RVE) concept which obviously does not exist in composites with localized defects that are considered in the present investigation) a rectangular region $-H \leqslant x_2 \leqslant H, -L \leqslant x_3 \leqslant L$ of the periodically layered piezoelectric composite is considered which includes the localized damaged region, see Fig. 1(b). This region is divided into $(2M_2 + 1)(2M_3 + 1)$ cells (Fig. 1(b) is shown for $M_2 = M_3 = 2$). Every cell is labeled by the pair (K_2, K_3) with $K_2 = -M_2, \ldots, M_2$ and $K_3 = -M_3, \ldots, M_3$. In each cell, local coordinates (x_2', x_3') are introduced whose origins are located at its center, Fig. 1(c).

The governing Eqs. (1) and (6) of the material within cell (K_2, K_3) take the form
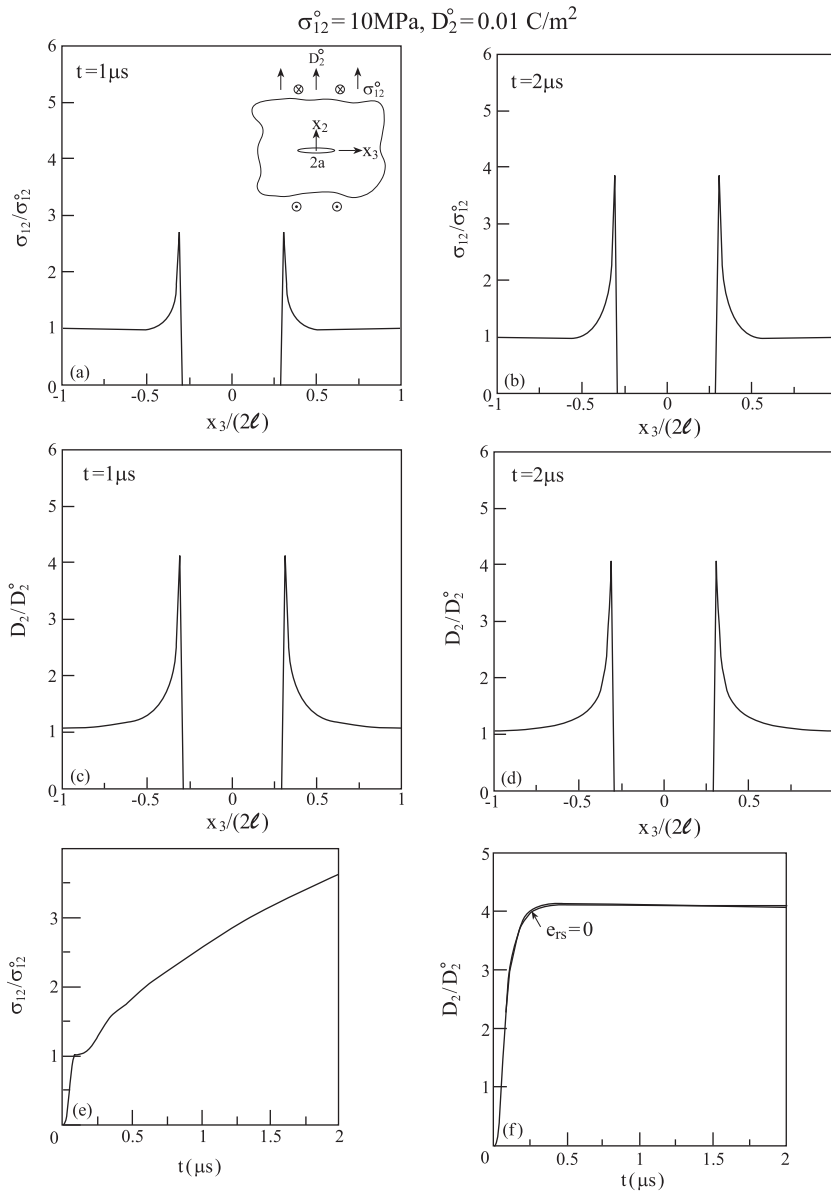
$$\sigma_{12}^\circ = 10\,\text{MPa},\ D_2^\circ = 0.01\ \text{C/m}^2$$

Fig. 4. The variations of the transverse shear stress and normal electric displacement along the crack line caused by the sudden appearance of of a crack $-0.3 \leqslant x_3/(2l) \leqslant 0.3$ caused by the application of initial field $\sigma_{12}^0 = 10$ MPa, $D_2^0 = 0.01$ C/m^2 in piezoelectric Cadmium Selenide material. (a) and (b) Transverse shear stress variations, (c) and (d) normal electric displacement variations. (e) and (f) The time variations of the transverse shear stress and normal electric displacement at the closest point ahead of the tip in the coupled and uncoupled cases.

$$\sigma_{jk,k}^{(K_2,K_3)} = \rho \frac{d^2}{dt^2} u_j^{(K_2,K_3)}, \quad j,k = 1,2,3 \tag{15}$$

$$D_{j,j}^{(K_2,K_3)} = 0, \quad j = 1,2,3 \tag{16}$$

The constitutive Eqs. (10) in the cell (K_2, K_3) can be written as

$$Y_r^{(K_2,K_3)} = \sum_{s=1}^{9} Z_{rs} X_s^{(K_2,K_3)} - Y_r^{e(K_2,K_3)}, \quad r = 1,\dots,9 \tag{17}$$

where the components of the eigen-electroelastic field in this cell are

$$Y_r^{e(K_2,K_3)} = \sum_{s=1}^{9} d_{rs} Z_{rs} X_s^{(K_2,K_3)}, \quad r = 1,\dots,9 \tag{18}$$

In order to formulate the continuity conditions that the various variables should fulfill, let us define the vectors $\boldsymbol{V}_m^{(K_2,K_3)}$:

$$\boldsymbol{V}_m^{(K_2,K_3)} = [u_{m1}, u_{m2}, u_{m3}, \sigma_{m1}, \sigma_{m2}, \sigma_{m3}, \psi, D_m]^{(K_2,K_3)}, \quad m = 2,3 \tag{19}$$

These vectors assemble the time-dependent components of the displacements $u_{m1}^{(K_2,K_3)}, u_{m2}^{(K_2,K_3)}, u_{m3}^{(K_2,K_3)}$, traction components $\sigma_{m1}^{(K_2,K_3)}$, $\sigma_{m2}^{(K_2,K_3)}, \sigma_{m3}^{(K_2,K_3)}$ on a plane perpendicular to the x_m-axis at the cell (K_2, K_3), as well as the electric potential $\psi^{(K_2,K_3)}$ and the electric displacements $D_m^{(K_2,K_3)}$ acting on these planes.

The continuity of displacements, tractions, electric potential and displacements between adjacent cells should be imposed. Thus,
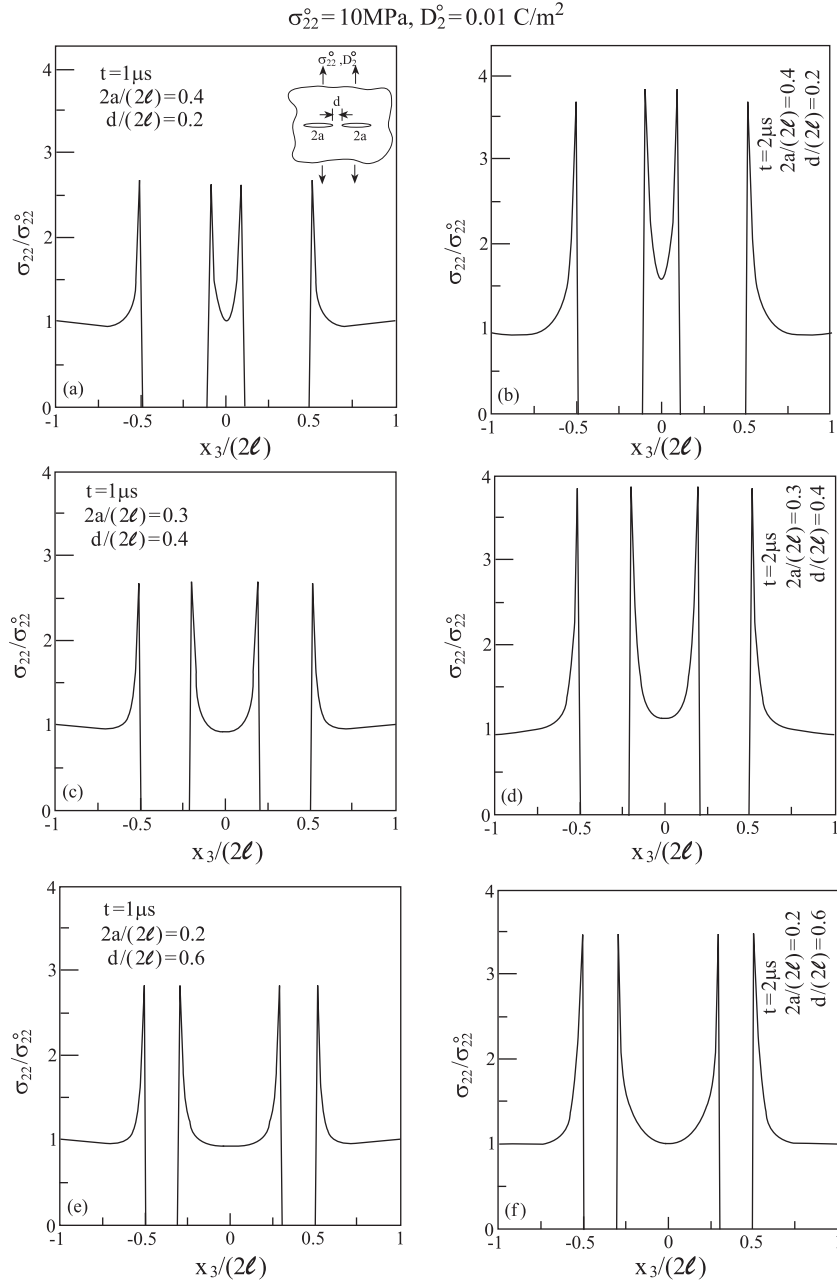
$\sigma_{22}^\circ = 10 \text{MPa},\ D_2^\circ = 0.01\ \text{C/m}^2$

Fig. 5. The piezoelectric Cadmium Selenide material is subjected to a combined electromechanical normal loading: $\sigma_{22}^0 = 10$ MPa, $D_2^0 = 0.01$ C/m². As a result, two interacting cracks appear which are characterized by: (a)-(b) $2a/(2l) = 0.4, d/(2l) = 0.2$, (c) and (d) $2a/(2l) = 0.3, d/(2l) = 0.4$, (e) and (f) $2a/(2l) = 0.2, d/(2l) = 0.6$. The figures show the variations at $t = 1$ and 2 μs of the normal stresses along the line of the cracks.

$$\left[\boldsymbol{V}_2(h, x_3', t) \right]^{(K_2, K_3)} - \left[\boldsymbol{V}_2(-h, x_3', t) \right]^{(K_2+1, K_3)} = 0 \qquad (20)$$

where $K_2 = -M_2, \ldots, M_2 - 1, K_3 = -M_3, \ldots, M_3, -l \leqslant x_3' \leqslant l$, and

$$\left[\boldsymbol{V}_3(x_2', l, t) \right]^{(K_2, K_3)} - \left[\boldsymbol{V}_3(x_2', -l, t) \right]^{(K_2, K_3+1)} = 0 \qquad (21)$$

where $K_2 = -M_2, \ldots, M_2, K_3 = -M_3, \ldots, M_3 - 1, -h \leqslant x_2' \leqslant h$.

In the following, the boundary conditions that specify the electro-elastic field at the opposite sides $x_2 = \pm H, x_3 = \pm L$ of the rectangle of Fig. 1(b) are presented. It is assumed that these boundaries are sufficiently far away from the localized defects so that the field there can be assumed to be periodic. Thus at any instant, the tractions at the opposite sides of the rectangular domain are equal:

$$\sigma_{2j}^{(M_2, K_3)}(h, x_3', t) - \sigma_{2j}^{(-M_2, K_3)}(-h, x_3', t) = 0,$$
$$K_3 = -M_3, \ldots, M_3, \ j = 1, 2, 3, \ -l \leqslant x_3' \leqslant l \qquad (22)$$

and

$$\sigma_{3j}^{(K_2, M_3)}(x_2', l, t) - \sigma_{3j}^{(K_2, -M_3)}(x_2', -l, t) = 0,$$
$$K_2 = -M_2, \ldots, M_2, \ j = 1, 2, 3, \ -h \leqslant x_2' \leqslant h \qquad (23)$$

Similarly, the electrical displacement at the opposite sides of the rectangular domain should be equal. Thus

$$D_2^{(M_2, K_3)}(h, x_3', t) - D_2^{(-M_2, K_3)}(-h, x_3', t) = 0,$$
$$K_3 = -M_3, \ldots, M_3, \ -l \leqslant x_3' \leqslant l \qquad (24)$$

$$\sigma_{22}^\circ = 10\text{MPa}, \ D_2^\circ = 0.01 \ \text{C/m}^2$$

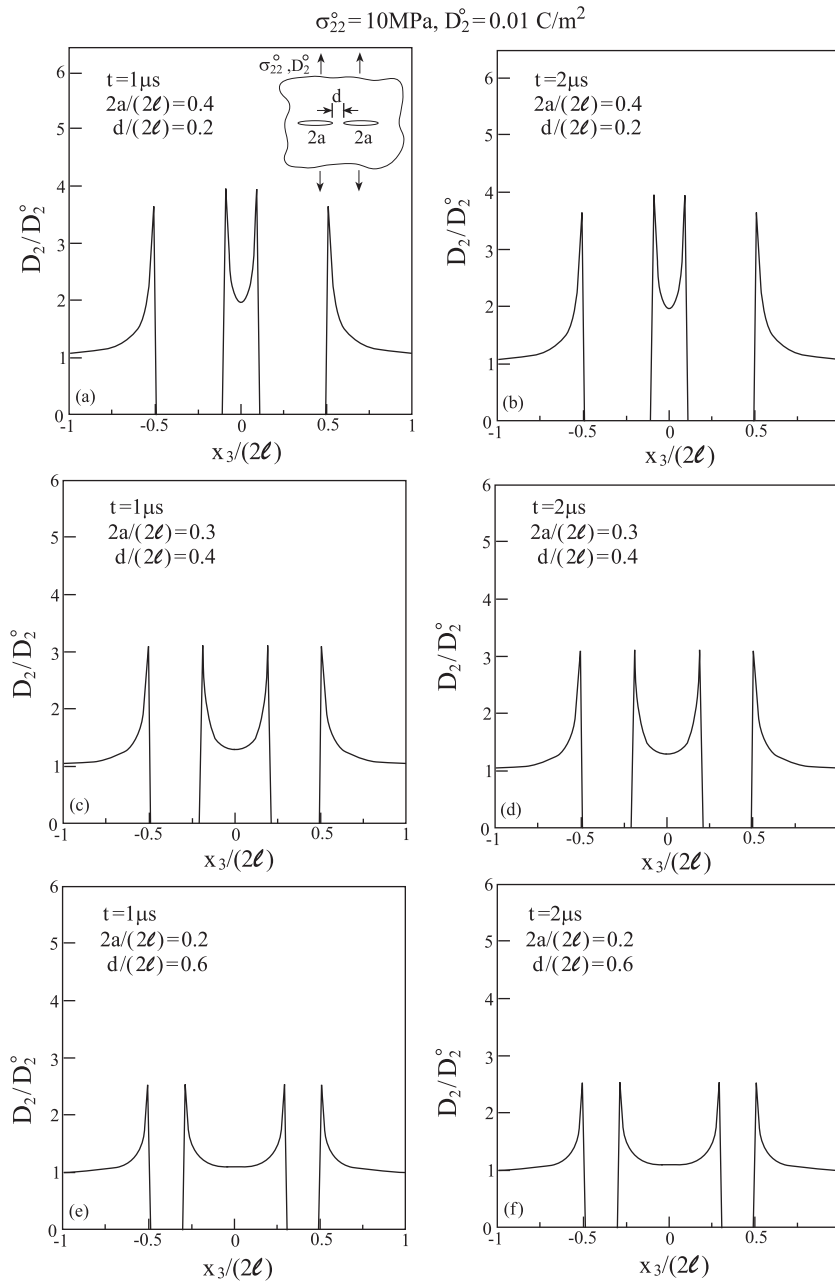**Fig. 6.** Same as Fig. 5 but for the variations of the electric displacements.

and

$$D_3^{(K_2,M_3)}(x_2',l,t) - D_3^{(K_2,-M_3)}(x_2',-l,t) = 0,$$
$$K_2 = -M_2,\ldots,M_2, \ -h \leqslant x_2' \leqslant h \tag{25}$$

In the presence of initial system of stresses σ_{jk}^0 and electrical displacements D_j^0, the mechanical displacements and electric potential at the opposite sides $\pm H$ and $\pm L$ are related by

$$\mathbf{u}^{(M_2,K_3)}(h,x_3',t) - \mathbf{u}^{(-M_2,K_3)}(-h,x_3',t) = 0,$$
$$K_3 = -M_3,\ldots,M_3, \ -l \leqslant x_3' \leqslant l \tag{26}$$

$$\mathbf{u}^{(K_2,M_3)}(x_2',l,t) - \mathbf{u}^{(K_2,-M_3)}(x_2',-l,t) = 0,$$
$$K_2 = -M_2,\ldots,M_2, \ -h \leqslant x_2' \leqslant h \tag{27}$$

$$\psi^{(M_2,K_3)}(h,x_3',t) - \psi^{(-M_2,K_3)}(-h,x_3',t) = 0,$$
$$K_3 = -M_3,\ldots,M_3, \ -l \leqslant x_3' \leqslant l \tag{28}$$

$$\psi^{(K_2,M_3)}(x_2',l,t) - \psi^{(K_2,-M_3)}(x_2',-l,t) = 0,$$
$$K_2 = -M_2,\ldots,M_2, \ -h \leqslant x_2' \leqslant h \tag{29}$$

The double discrete Fourier of the displacement vector $\mathbf{u}^{(K_2,K_3)}$ (for example) is defined by

$$\hat{\mathbf{u}}(x_2',x_3',\phi_p,\phi_q,t) = \sum_{K_2=-M_2}^{M_2} \sum_{K_3=-M_3}^{M_3} \mathbf{u}^{(K_2,K_3)}(x_2',x_3',t)$$
$$\times \exp\left[i(K_2\phi_p + K_3\phi_q)\right] \tag{30}$$

where

$$\sigma_{22}^{\circ} = 10\,\text{MPa},\ D_2^{\circ} = 0.01\ \text{C/m}^2$$
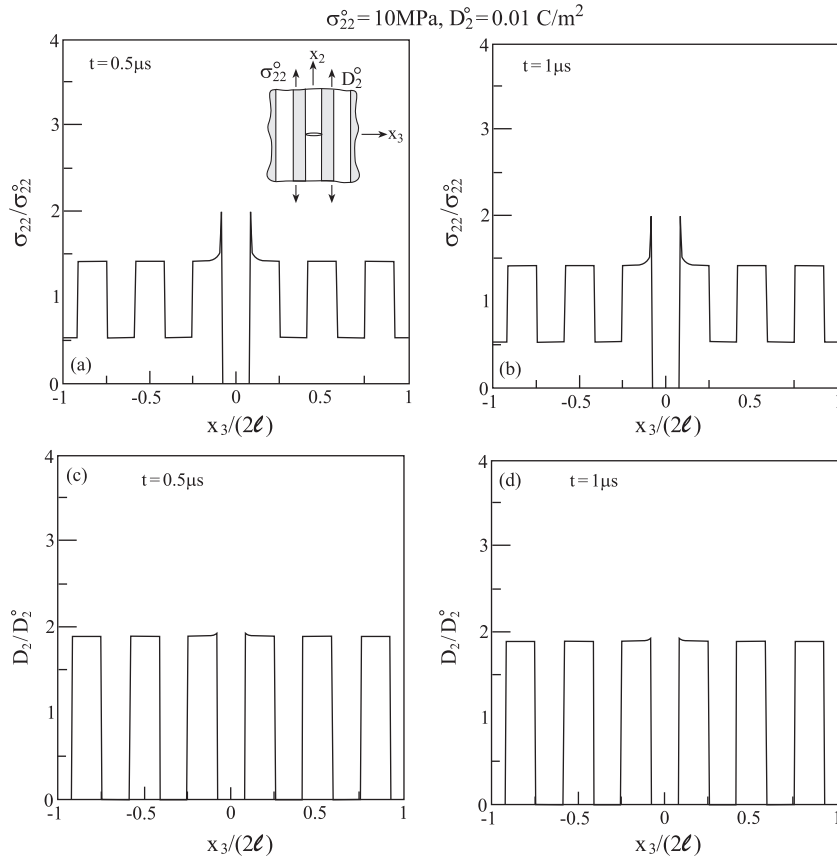

Fig. 7. A piezoelectric BaTiO$_3$/Cadmium Selenide layered composite is subjected to a combined electromechanical normal loading: $\sigma_{22}^0 = 10\,\text{MPa}, D_2^0 = 0.01\ \text{C/m}^2$. The variations of the (a) and (b) normal stresses, and (c)-(d) electrical displacements along x_3 at $x_2 = 0$ caused by the sudden breakage of a single Cadmium Selenide layer at $t = 0$.

$$\phi_p = \frac{2\pi p}{2M_2 + 1}, \quad p = 0, \pm1, \pm2, \ldots, \pm M_2, \quad \phi_q = \frac{2\pi q}{2M_3 + 1},$$
$$q = 0, \pm1, \pm2, \ldots, \pm M_3,$$

The application of this transform to the boundary problem (15)–(21) for the rectangular domain $-H < x_2 < H, -L < x_3 < L$, divided into $(2M_2 + 1)(2M_3 + 1)$ cells, converts it to the problem for the single representative cell $-h < x_2' < h, -l < x_3' < l$ with respect to the complex valued transforms. The governing electro-elastic and constitutive equations have the form

$$\hat{\sigma}_{jk,k} = \rho \frac{d^2}{dt^2}\hat{u}_j, \quad j, k = 1, 2, 3 \tag{31}$$

$$\hat{D}_{j,j} = 0, \quad j = 1, 2, 3 \tag{32}$$

and

$$\hat{Y}_r = \sum_{s=1}^{9} Z_{rs}\hat{X}_s - \hat{Y}_r^e, \quad r = 1, \ldots, 9 \tag{33}$$

where the components of the transformed eigen-field vector components are given by

$$\hat{Y}_r^e = \sum_{s=1}^{9} Z_{rs}d_{rs}\hat{X}_s \tag{34}$$

The conditions relating the opposite sides of the representative cell, Eq. (22)–(29), take the form

$$\hat{\sigma}_{2j}(h, x_3', t) = \exp(-i\phi_p)\hat{\sigma}_{2j}(-h, x_3', t), \quad -l \leqslant x_3' \leqslant l,$$
$$j = 1, 2, 3 \tag{35}$$

$$\hat{u}(h, x_3', t) = \exp(-i\phi_p)\hat{u}(-h, x_3', t), \quad -l \leqslant x_3' \leqslant l \tag{36}$$

$$\hat{D}_2(h, x_3', t) = \exp(-i\phi_p)\hat{D}_2(-h, x_3', t), \quad -l \leqslant x_3' \leqslant l, \tag{37}$$

$$\hat{\psi}(h, x_3', t) = \exp(-i\phi_p)\hat{\psi}(-h, x_3', t), \quad -l \leqslant x_3' \leqslant l \tag{38}$$

and

$$\hat{\sigma}_{3j}(x_2', l, t) = \exp(-i\phi_q)\hat{\sigma}_{3j}(x_2', -l, t), \quad -h \leqslant x_2' \leqslant h,$$
$$j = 1, 2, 3 \tag{39}$$

$$\hat{u}(x_2', l, t) = \exp(-i\phi_q)\hat{u}(x_2', -l, t), \quad -h \leqslant x_2' \leqslant h \tag{40}$$

$$\hat{D}_3(x_2', l, t) = \exp(-i\phi_q)\hat{D}_3(x_2', -l, t), \quad -h \leqslant x_2' \leqslant h, \tag{41}$$

$$\hat{\psi}(x_2', l, t) = \exp(-i\phi_q)\hat{\psi}(x_2', -l, t), \quad -h \leqslant x_2' \leqslant h \tag{42}$$

where $p = -M_2, \ldots, M_2, q = -M_3, \ldots, M_3$.

3.2. Wave propagation in piezoelectric composites analysis

The representative cell initial-boundary value problem (31)–(42), formulated in the transform domain where the identity of the cells disappeared, is solved by employing the analysis for wave propagation in piezoelectric composite materials. For perfectly elastic composites this analysis was is described in Aboudi et al. (2013) and it has been modified by Aboudi (2013a) to incorporate the effects of initial stresses and eigen-stresses. Presently it is necessary to generalize this analysis to incorporate the electrical effects that exists due to the piezoelectric behavior of the phases.

According to this theory, the domain $-h \leqslant x_2' \leqslant h, -l \leqslant x_3' \leqslant l$ (the representative cell) is divided into several rectangular subcells, see Fig. 1(c). The transformed time-dependent mechanical

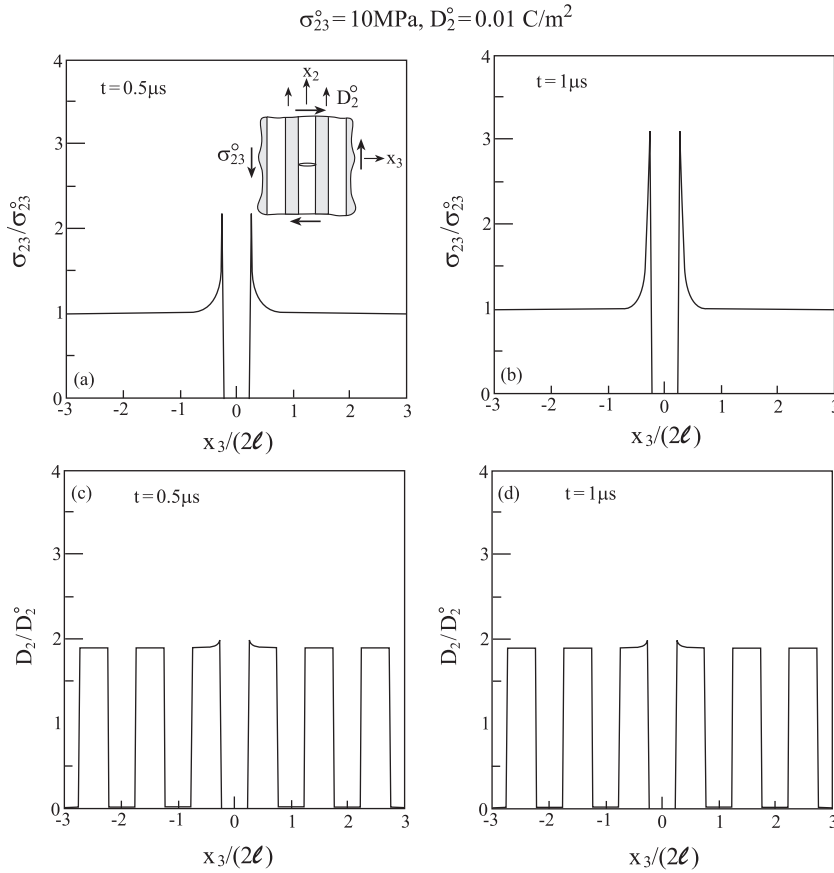$$\sigma_{23}^{\circ} = 10\text{MPa},\ D_2^{\circ} = 0.01\ \text{C/m}^2$$

Fig. 8. A piezoelectric BaTiO$_3$/Cadmium Selenide layered composite is subjected to a combined axial shear mechanical and normal electrical loading: $\sigma_{23}^0 = 10$ MPa, $D_2^0 = 0.01$ C/m^2. The variations of the (a) and (b) axial shear stresses, and (c)-(d) normal electrical displacements along x_3 at $x_2 = 0$ caused by the sudden breakage of a single Cadmium Selenide layer at $t = 0$.

displacements and electric potential are expanded into a second-order polynomials, and the transformed governing equations, interfacial and boundary conditions are imposed in the average (integral) sense. As a result, a system of ordinary differential equations is obtained whose solution determine at any instant the field variables in the transform domain. The analysis for the inclusion of the electrical field (which complements the elastodynamic one presented in Aboudi (2013a)) is described the Appendix. As a result of the imposed initial stress $\boldsymbol{\sigma}^0$ and electric displacement $\boldsymbol{D}^0$, this analysis requires the knowledge of the resulting strains $\boldsymbol{\epsilon}^0$ and electric field $\boldsymbol{E}^0$ in the phases caused by these externally applied loadings.

1. For a homogeneous piezoelectric material with localized defects, $\boldsymbol{\epsilon}^0$ and $\boldsymbol{E}^0$ are simply given by the inversion of the constitutive Eqs. (2) and (7). From these relations the expressions for $\hat{\boldsymbol{\epsilon}}^0$ and $\hat{\boldsymbol{E}}^0$ in the transform domain can be readily established.

2. For a periodically layered piezoelectric composite, the resulting normal strains and electric field $E_3^{0)}$ in the two layers (labeled by f and m) are determined from the following conditions (see Fig. 1(a)).

$$
\begin{aligned}
\epsilon_{11}^{0(f)} &= \epsilon_{11}^{0(m)} \\
\epsilon_{22}^{0(f)} &= \epsilon_{22}^{0(m)} \\
\sigma_{33}^{0(f)} &= \sigma_{33}^{0(m)} = \sigma_{33}^0 \\
t_f\sigma_{11}^{0(f)} + t_m\sigma_{11}^{0(m)} &= (t_f + t_m)\sigma_{11}^0 \\
t_f\sigma_{22}^{0(f)} + t_m\sigma_{22}^{0(m)} &= (t_f + t_m)\sigma_{22}^0 \\
D_3^{0(f)} &= D_3^{0(m)} = D_{33}^0
\end{aligned}
\tag{43}
$$

These relations form a system of 8 equations in the unknown normal strains and electric field $E_3^{0(f)}, E_3^{0(m)}$ in the layers. In addition,

$$
\begin{aligned}
\sigma_{23}^{0(f)} &= \sigma_{23}^{0(m)} = \sigma_{23}^0 \\
E_2^{0(f)} &= E_2^{0(m)} \\
t_f D_2^{0(f)} + t_m D_2^{0(m)} &= (t_f + t_m)D_2^0
\end{aligned}
\tag{44}
$$

These form a system of 4 equations in the unknown axial shear strains ϵ_{23}^0 and electric field E_2^0 in the layers. Finally,

$$
\begin{aligned}
\sigma_{13}^{0(f)} &= \sigma_{13}^{0(m)} = \sigma_{13}^0 \\
E_1^{0(f)} &= E_1^{0(m)} \\
t_f D_1^{0(f)} + t_m D_1^{0(m)} &= (t_f + t_m)D_1^0
\end{aligned}
\tag{45}
$$

which forms a system of 4 equations in the unknown axial shear strains ϵ_{13}^0 and electric field E_1^0 in the layers. As to the transverse shear strains $\epsilon_{12}^{0(f)}$ and $\epsilon_{12}^{0(m)}$ in the layers, they can be readily determined from

$$
\epsilon_{12}^{0(f)} = \epsilon_{12}^{0(m)} = \frac{\sigma_{12}^0}{2G_T^*}
\tag{46}
$$

where $G_T^* = (t_f C_{66}^{(f)} + t_m C_{66}^{(m)})/(t_f + t_m)$, being the effective transverse shear modulus of the composite. Thus from these relations the expressions for $\hat{\boldsymbol{\epsilon}}^0$ and $\hat{\boldsymbol{E}}^0$ in the layers in the transform domain can be readily determined.

It is possible to represent the resulting induced strains and electric field in the layers in the form
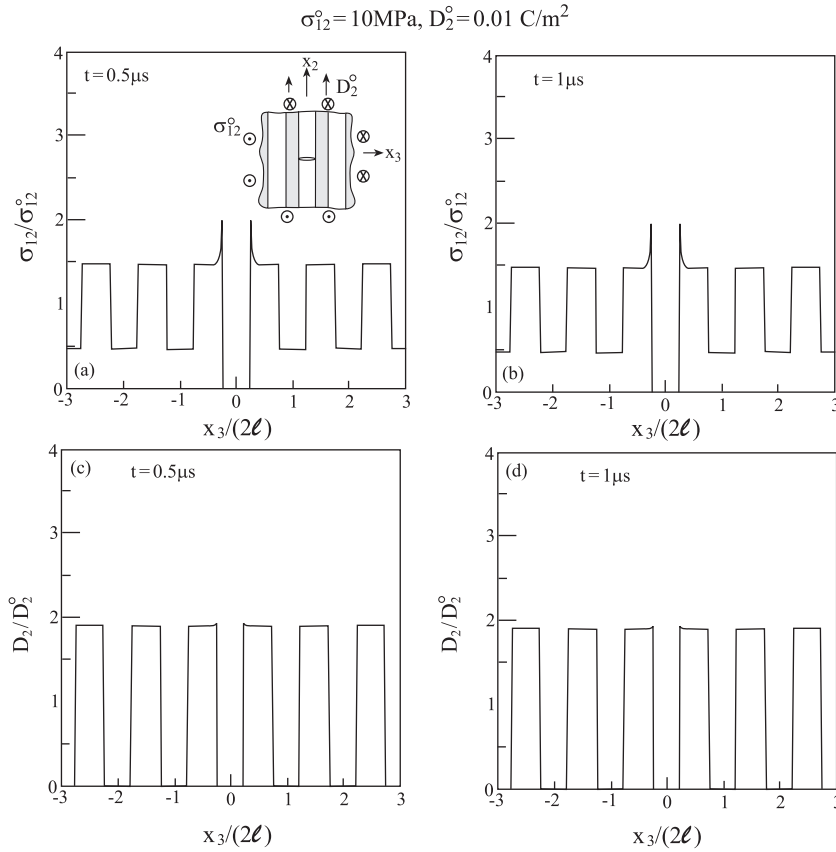
$\sigma_{12}^\circ = 10 \text{MPa}, D_2^\circ = 0.01 \text{ C/m}^2$

Fig. 9. A piezoelectric BaTiO₃/Cadmium Selenide layered composite is subjected to a combined transverse shear mechanical and normal electrical loading: $\sigma_{12}^0 = 10$ MPa, $D_2^0 = 0.01$ C/m². The variations of the (a) and (b) transverse shear stresses, and (c) and (d) normal electrical displacements along x_3 at $x_2 = 0$ caused by the sudden breakage of a single Cadmium Selenide layer at $t = 0$.

$$\left\{ \begin{array}{c} \boldsymbol{\epsilon}^{0(p)} \\ \boldsymbol{E}^{0(p)} \end{array} \right\} = \boldsymbol{A}^{(p)} \left\{ \begin{array}{c} \boldsymbol{\sigma}^0 \\ \boldsymbol{D}^0 \end{array} \right\}, \quad p = f, m \tag{47}$$

where $\boldsymbol{A}^{(p)}$ is referred to as the concentration tensors of the piezoelectric layered composite. They relate the induced strains and electric field layers $p = f, m$ to the externally applied stresses and electric displacements on the composite. These tensors can be easily related to the conventional strain and stress concentration tensors.

3. For fiber-reinforced piezoelectric composites that are subjected to an initial system of stresses and electrical displacements, the resulting strains and electric field in the constituents can be determined by employing a micromechanical analysis (e.g., Aboudi (2001)) that provides the concentration tensors $\boldsymbol{A}^{(phase)}$ which relate the strains and electrical field in the fiber and matrix phases to the externally applied stresses and electrical displacements.

3.3. Solution procedure

The time-dependent electro-mechanical field response is determined as follows. Assume that all the electro-mechanical field variables at time t have been determined.

1. The mechanical field variables at time $t + \Delta t$ (where Δt is a time increment) are determined by integrating the evolution equations (A.54) of Aboudi (2013a) (see this reference for more details about the construction of these equations in which the electric effects should be incorporated).

2. With the established mechanical field, the electrical field variables are obtained by solving the algebraic system of Eq. (A.29) at this time.

3. Once the solution for all electro-mechanical field variables in the transform domain at time $t + \Delta t$ have been established, the actual electro-elastic field can be readily determined at any point in cell (K_2, K_3) of the considered rectangular region $-H \leqslant x_2 \leqslant H, -L \leqslant x_3 \leqslant L$ by the inverse transform formula. For the mechanical displacements, for example, this formula is given by:

$$\boldsymbol{u}^{(K_2, K_3)}(x_2', x_3', t) = \frac{1}{(2M_2 + 1)(2M_3 + 1)}$$
$$\times \sum_{p=-M_2}^{M_2} \sum_{q=-M_3}^{M_3} \hat{\boldsymbol{u}}(x_2', x_3', \phi_p, \phi_q, t)$$
$$\times \exp\left[-i(K_2\phi_p + K_3\phi_q)\right] \tag{48}$$

4. The right-hand-side vector $\boldsymbol{N}(t + \Delta t)$ of Eq. (A.29) involves the eigen-electrical field $\boldsymbol{D}^e(t + \Delta t)$ which are not known. Hence an iterative procedure is required according to which the 2nd and 3rd step are repeated until a convergent solution is achieved.

The verification of the procedure and results that are presented in the following were carried out by discretizing the representative cell, Fig. 1(c), into $N_\beta = N_\gamma = 50$ subcells. These results are given for BaTiO₃ and Cademium Selenide piezoelectric materials whose properties are given in Tables 1 and 2, (Qin,
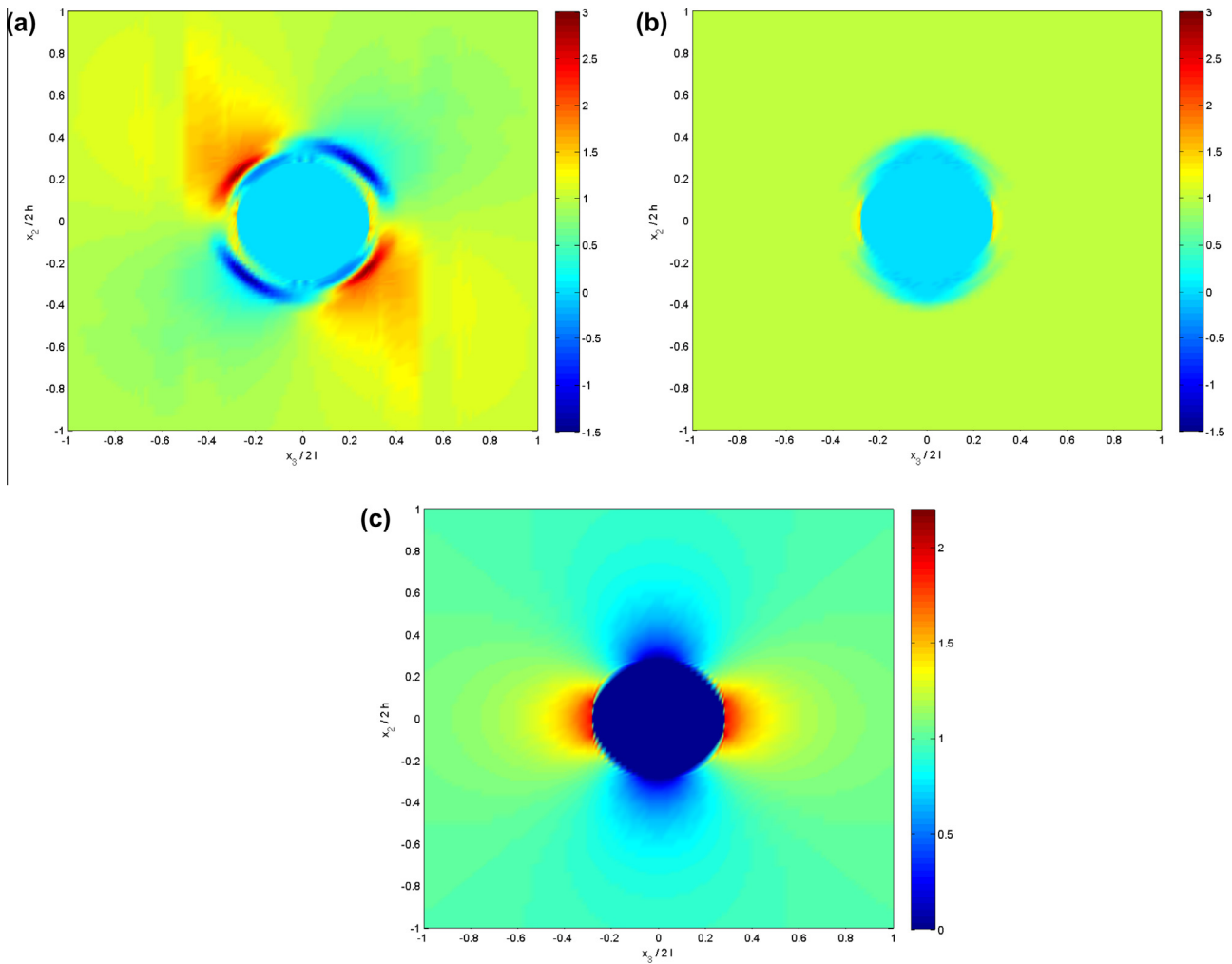
Fig. 10. Field distribution at $t = 1$ μs in the plane $-1 \leqslant x_2/(2h) \leqslant 1, -1 \leqslant x_3/(2l) \leqslant 1$, caused by the sudden formation of a cavity in an initially loaded Cadmium Selenide piezoelectric material by a combined electromechanical stress $\sigma_{22}^0 = 10$ MPa and electrical displacement $D_2^0 = 0.01$ C/m². (a) The distribution of the normal stress $\sigma_{22}/\sigma_{22}^0$, (b) the distribution of the normal stress $\sigma_{22}/\sigma_{22}^0$ in the corresponding uncoupled case, (c) the distribution of the normal electrical displacement D_2/D_2^0.

2001). The electromechanical loading is characterized by a stress of 10 MPa and electric displacement of 0.01 C/m². These values are within the range mentioned by Pak (1992) and Sosa (1991). It should be noted that except in the Verification section where the poling of the piezoelectric material is oriented in the x_1-direction, in all other cases the poling is directed in the x_3-direction. Finally, it should be remarked that in all cases presented in the following in which the responses to the sudden appearance of cracks are dealt with, impermeable boundary conditions have been imposed. Impermeable boundary conditions assume that the upper and lower surfaces of the crack are free of surface tractions and surface charge, cf. Pak (1990) for example. This author presented in a static problem an analytical solution of a crack under anti-plane mechanical loading in a piezoelectric material, and also discussed the issue of boundary conditions on piezoelectric crack surfaces. The present method however can be also applied in the cases of permeable boundary conditions. This has been demonstrated by Aboudi (2013b) in the static cases. As mentioned previously, the present approach ultimately employs a discretization procedure, hence it should not be expected to yield a mathematical singularity at the tip of the cracks.

4. Verification

In the elastic case, (Aboudi, 2013a), it was possible to verify the proposed analysis of wave propagation in periodic composites with a localized defect by comparisons with analytical solutions for the sudden appearance of cracks in Mode I, (Baker, 1962), and III, (Freund, 1990), deformation; the sudden formation of a cavity, (Miklowitz, 1960); and the diffraction of horizontally shear waves in a material by a semi-infinite crack, (Achenbach, 1973). In the absence of electro-mechanical coupling ($e_{rs} = 0$), these verifications are valid of course here too. In the present electro-mechanical case, an analytical solution is available for the transient response of a piezoelectric material with a semi-infinite mode-III crack to impact, (Li, 2001). This analytical solution was established for a piezoelectric material whose poling (axis of symmetry) is oriented in the x_1-direction and with the crack's leading edges parallel to the poling direction. Hence Eq. (2) and (7) are given in the present case (only) by

$$\sigma_{12} = 2c_{66}\epsilon_{12} - e_{15}E_2, \quad \sigma_{13} = 2c_{66}\epsilon_{13} - e_{15}E_3,$$
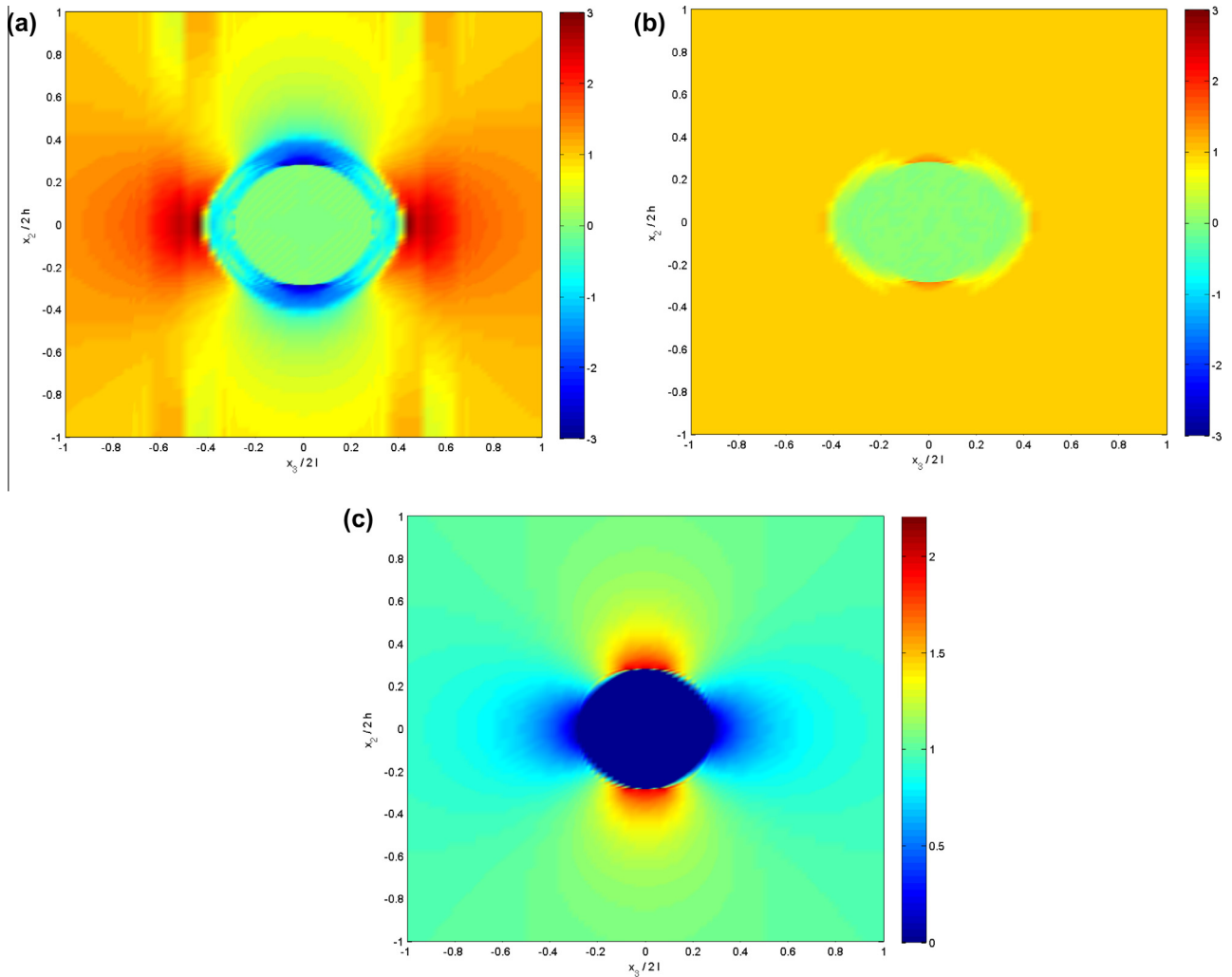$$D_2 = 2e_{15}\epsilon_{12} + \kappa_{11}E_2, \quad D_3 = 2e_{15}\epsilon_{13} + \kappa_{11}E_3 \quad (49)$$

Fig. 11. Field distribution at $t = 1$ μs in the plane $-1 \leqslant x_2/(2h) \leqslant 1, -1 \leqslant x_3/(2l) \leqslant 1$, caused by the sudden formation of a cavity in an initially loaded Cadmium Selenide piezoelectric material by a combined electromechanical stress $\sigma_{33}^0 = 10$ MPa and electrical displacement $D_3^0 = 0.01$ C/m². (a) The distribution of the normal stress $\sigma_{33}/\sigma_{33}^0$, (b) the distribution of the normal stress $\sigma_{33}/\sigma_{33}^0$ in the corresponding uncoupled case, (c) the distribution of the normal electrical displacement D_3/D_3^0.

Consider a semi-infinite crack $x_3 \leqslant 0$ that is impacted by a concentrated combined electro-mechanical loadings located at $x_3 = -b$ which are given by

$$\sigma_{12}(x_2 = 0, x_3, t) = -P\delta(x_3 + b), \quad D_2(x_2 = 0, x_3, t)$$
$$= -Q\delta(x_3 + b), \quad t > 0 \tag{50}$$

where P and Q are constants and $\delta(.)$ is the Dirac delta function. The transient strain response along the crack line is given by

$$\epsilon_{12}(x_2 = 0, x_3, t) = \frac{\kappa_{11}P + e_{15}Q}{2(c_{66}\kappa_{11} + e_{15}^2)} \frac{1}{\pi(x_3 + b)} \sqrt{\frac{b}{x_3}}, \quad 0 < x_3 < c_s t - b$$

$$\epsilon_{12}(x_2 = 0, x_3, t) = 0, \quad x_3 > c_s t - b \tag{51}$$

where $c_s = \sqrt{(c_{66} + e_{15}^2/\kappa_{11})/\rho}$ is the shear wave velocity in the piezoelectric material. This strain component vanishes when $x_3 > c_s t - b$ since at these locations shear waves do no arrive.

This solution can be employed as a Green's function for this semi-infinite crack, but impacted this time by the combined loading (50) along its entire surface $x_3 \leqslant 0$. Since the strains at point $(0, x_3)$ will be influenced by all loadings from $b = 0$ to

$b = c_s t - x_3$, the resulting response is given by integrating Eq. (51) with respect to b from $b = 0$ to $b = c_s t - x_3$. This yields, (Li, 2001):

$$\epsilon_{12}(x_2 = 0, x_3, t)$$
$$= \frac{\kappa_{11}P + e_{15}Q}{\pi(c_{66}\kappa_{11} + e_{15}^2)} \left(\sqrt{\frac{c_s t - x_3}{x_3}} - \tan^{-1}\sqrt{\frac{c_s t - x_3}{x_3}} \right) \tag{52}$$

In Fig. 2(a) and (b), comparisons between this analytical and present solution approach for the response along the crack line to the sudden appearance of a semi-infinite crack $x_3/(2l) \leqslant 0.3$ in Cadmium Selenide caused by initially applied stress $\sigma_{12}^0 = 10 MPa$ and electric displacement $D_2^0 = 0.01$ C/m² (which corresponds to the values of P and Q, respectively) are shown at $t = 1$ and $t = 2$ μs. The resulting initial strain and electric field are: $\epsilon_{12}^0 = 1\%$, $E_2^0 = 1.19$ V/m. Good agreement between the analytical solution (51) (which exhibits of course a singularity at the crack's tip), to which the far-field has been superimposed to obtain traction and electrical displacement free surfaces, and the present approach can be observed. In Fig. 2(c) and (d), the same comparisons are given in the uncoupled case (i.e., $e_{15} = 0$). Here the applied initially applied loading results in $\epsilon_{12}^0 = 0.04\%, E_2^0 = 1.23$ V/m. The lower
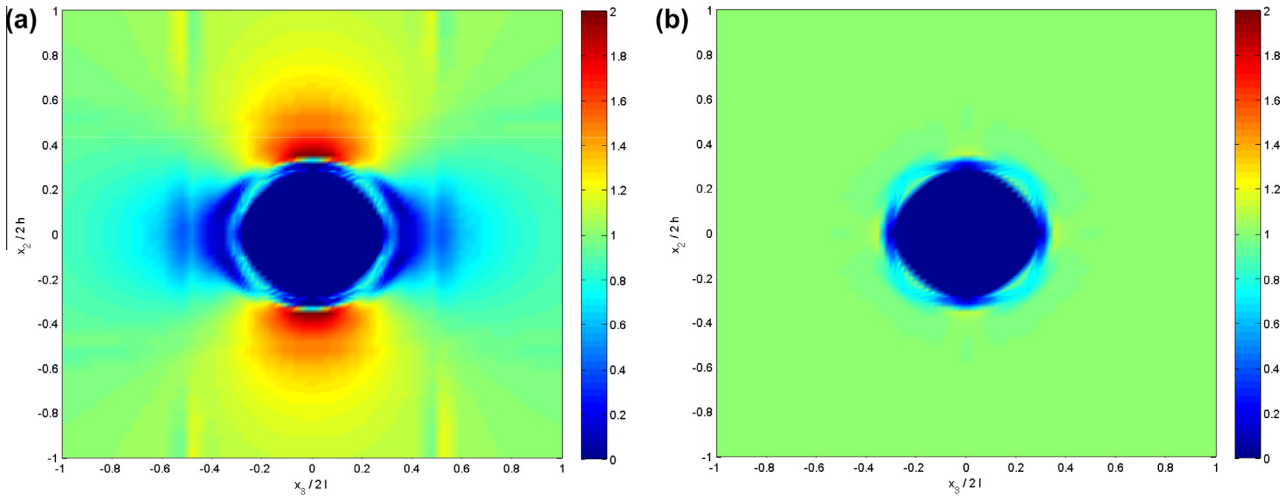
Fig. 12. Field distribution at $t = 1$ μs in the plane $-1 \leqslant x_2/(2h) \leqslant 1, -1 \leqslant x_3/(2l) \leqslant 1$, caused by the sudden formation of a cavity in an initially loaded Cadmium Selenide piezoelectric material by a combined electromechanical stress $\sigma_{23}^0 = 10$ MPa and electrical displacement $D_2^0 = 0.01$ C/m². (a) The distribution of the axial shear stress $\sigma_{23}/\sigma_{23}^0$, (b) the corresponding distribution in the uncoupled case.

values of shear stresses at the closest point to the crack's tip in the absence of coupling as compared with the coupled case should be noted.

5. Applications

5.1. The sudden formation of a crack caused by combined initial electromechanical loadings

Consider a crack of length $2a/(2l) = 0.6$, extending along $-0.3 \leqslant x_3/(2l) \leqslant 0.3$, embedded in Cadmium Selenide piezoelectric material. This material is initially subjected to a combined normal loading $\sigma_{22}^0 = 10$ MPa, $D_2^0 = 0.01$ C/m². The leading edge of the crack extends in the x_1-direction normal to the poling. The resulting non-vanishing initial strains and electric field are: $\epsilon_{11}^0 = -0.01\%, \epsilon_{22}^0 = 0.02\%, \epsilon_{33}^0 = -0.005\%, \epsilon_{23}^0 = 0.06\%, E_2^0 = 1.2$ V/m, $E_3^0 = 0.004$ V/m. In the uncoupled case the same order of magnitudes of strains is obtained, but with $\epsilon_{23}^0 = E_3^0 = 0$. Thus, additional field components emerge caused by the electromechanical coupling. Fig. 3(a)–(d) exhibit the resulting normal stress and electrical

displacements along the crack line caused by the application of this combined electromechanical loading at $t = 1$ and $t = 2$ μs. The effect of coupling on the resulting field in this case appears to be inappreciable. This is exhibited in Fig. 3(e) and (f) by recording the time variations of normal stress and electrical displacements at the closest point ahead of the crack's tip. The effect of coupling, on the other hand, can be detected by examining the axial shear component σ_{23}. It turns out that at $t = 2$ μs, $\sigma_{23}/\sigma_{22}^0$ varies between -1.8 MPa and 2 MPa in the coupled case as against -0.8 MPa to 0.8 MPa in the uncoupled case. Hence this component forms a good indicator for the existence of coupling. In contrast, identical variations of the electrical displacement component -2.7 C/m² $\leqslant D_3/D_2^0 \leqslant 2.7$ C/m² are observed at $t = 2$ μs. This is due to the small induced strains which do not affect the electric field under these two circumstances.

Next, consider the case when the Cadmium Selenide piezoelectric material is initially loaded by $\sigma_{12}^0 = 10$ MPa (transverse shear) and $D_2^0 = 0.01$ C/m² which causes the appearance of a crack extending along $-0.3 \leqslant x_3/(2l) \leqslant 0.3$. Here, the non-vanishing field components are: $\epsilon_{12}^0 = 0.03\%, \epsilon_{23}^0 = 0.06\%, E_2^0 = 1.2$ V/m. In the
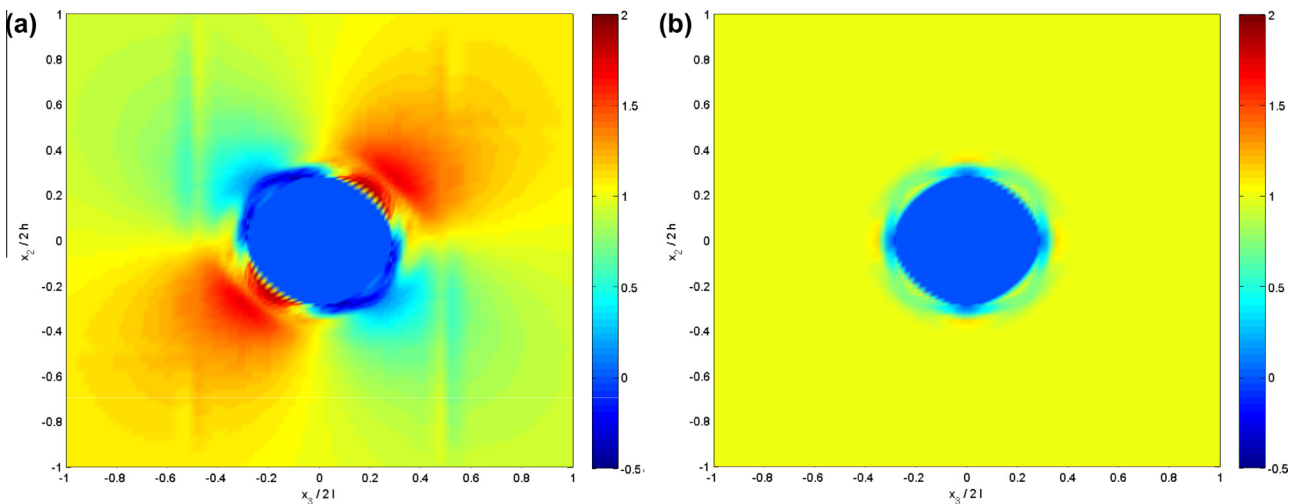
Fig. 13. Field distribution at $t = 1$ μs in the plane $-1 \leqslant x_2/(2h) \leqslant 1, -1 \leqslant x_3/(2l) \leqslant 1$, caused by the sudden formation of a cavity in an initially loaded Cadmium Selenide piezoelectric material by a combined electromechanical stress $\sigma_{23}^0 = 10$ MPa and electrical displacement $D_3^0 = 0.01$ C/m². (a) The distribution of the axial shear stress $\sigma_{23}/\sigma_{23}^0$, (b) the corresponding distribution in the uncoupled case.

uncoupled case on the other hand: $\epsilon_{23}^0 = 0$. Fig. 4(a)–(d) exhibit the shear stress and normal electric displacement along the crack's line at $t = 1$ and $t = 2\,\mu s$. Similarly Fig. 4(e) and (f) show a comparison between the latter temporal field component variations at the closest point ahead of the crack's tip obtained in the coupled and uncoupled cases. Here too, the effect of the electromechanical coupling the stress component σ_{12} and electric components D_2, D_3 is negligible. But its effect on the induced normal and axial shear stress components σ_{22} and σ_{23} is tremendous. Here at $t = 2\,\mu s, -1.3\,\text{MPa} \leqslant \sigma_{22}/\sigma_{12}^0 \leqslant 1.4\,\text{MPa}$ and $-1.7\,\text{MPa} \leqslant \sigma_{23}/\sigma_{12}^0 \leqslant 2\,\text{MPa}$ in the coupled case, whereas $\sigma_{22} = 0$ and $\sigma_{23} = 0$ in the absence of coupling.

Finally, we consider the Cadmium Selenide piezoelectric material which is initially loaded by $\sigma_{22}^0 = 10\,\text{MPa}$ and $D_2^0 = 0.01\,\text{C/m}^2$. It is assumed that this loading causes the creation of two interacting cracks as shown in the inset to Fig. 5(a). Here too, the two cracks leading edges are in the perpendicular to the poling x_3-direction. Three cases are considered in which the crack's length and distances between the tips are: $2a/(2l) = 0.4, d/(2l) = 0.2; 2a/(2l) = 0.3, d/(2l) = 0.4$, and $2a/(2l) = 0.2, d/(2l) = 0.6$. The resulting normal stress and electric displacement along the crack's line are shown in Fig. 5 and 6 at time $t = 1$ and $t = 2\,\mu s$. The effect on the resulting field caused by the formation of the two cracks is clearly shown by the graphs of these figures.

5.2. Electromechanically initially loaded BaTiO$_3$/Cadmium Selenide layered composite: the effect of the sudden breakage of a single layer

Consider a periodically layered BaTiO$_3$/Cadmium Selenide composite that is subjected to initial combined electromechanical loadings, see Fig. 1(a). The layers are of equal widths $t_f = t_m$ where $t_f + t_m = 2l$. Suppose that at time $t = 0$ a single Cadmium Selenide layer has been suddenly broken as a result of which the transient response is sought. The length of the crack is $2a = t_m$.

In Fig. 7–9 the transient behavior of the stresses and electrical displacements are shown along the crack's line for the following initial types of combined loadings: $\sigma_{22}^0 = 10\,\text{MPa}, D_2^0 = 0.01\,\text{C/m}^2$ (normal loading); $\sigma_{23}^0 = 10\,\text{MPa}, D_2^0 = 0.01\,\text{C/m}^2$ (axial shear mechanical loading); and $\sigma_{12}^0 = 10\,\text{MPa}, D_2^0 = 0.01\,\text{C/m}^2$ (transverse shear mechanical loading), respectively, at two instances: $t = 0.5$ and $1\,\mu s$. As in the previous cases, the electrical displacements in the vicinity of the crack maintain (unlike the stresses) their value and do not increase with time. The effect of electromechanical coupling on the induced stress components has been also investigated. It turns out that in all these three types of loading this effect is not pronounced. Thus the induced axial shear stress σ_{23} in both the normal loading and transverse shear mechanical loading cases, as well as the induced normal stress σ_{22} in transverse shear mechanical loading case, were either not sensitive to the coupling or negligibly small.

5.3. The sudden formation of a cavity caused by combined initial electromechanical loadings

As discussed, the effect of the electromechanical coupling in all the previously examined cases with cracks was quite minor. Presently, we consider the sudden formation at $t = 0$ of a circular cavity in Cadmium Selenide piezoelectric material which was initially loaded by a combined electromechanical loading. The radius of the cavity is $R/(2l) = 0.282$ which forms an area of $0.25/(2l)^2$. As will be shown, the effect of electromechanical coupling in the present case is significant. We start by applying the initial electromechanical normal loading $\sigma_{22}^0 = 10\,\text{MPa}, D_2^0 = 0.01\,\text{C/m}^2$ perpendicular to the x_3 poling direction. Fig. 10(a) shows the stress $\sigma_{22}/\sigma_{22}^0$ distribution at time $t = 1\,\mu s$ in the plane

$-1 \leqslant x_2/(2h) \leqslant 1, -1 \leqslant x_3/(2l) \leqslant 1$ caused the sudden formation of the cavity. The corresponding uncoupled case ($e_{rs} = 0$) is shown in Fig. 10(b). It can be readily observed that the effect of coupling is significant. Actually, the distribution of the stresses in Fig. 10(b) are limited in the range $0 \leqslant \sigma_{22}/\sigma_{22}^0 \leqslant 1.5$ but the scale has been kept to confirm with that of Fig. 10(a). This well indicates the severity of the coupling effects. Finally, Fig. 10(c) exhibits the electric displacement distribution D_2/D_2^0. Here the effect of the coupling is negligible which implies that the strains are too small to affect the electric field.

The next case of a sudden cavity formation is when the piezoelectric material is initially loaded by $\sigma_{33}^0 = 10\,\text{MPa}$, $D_3^0 = 0.01\,\text{C/m}^2$ in the other normal direction which is parallel to the poling direction. Here the stress $\sigma_{33}/\sigma_{33}^0$ variations are shown in Fig. 11(a) and (b) in the coupled and uncoupled case at $t = 1\,\mu s$. As in the previous case, the effect of coupling is remarkable. The electric displacement distribution D_3/D_3^0 is shown in Fig. 11(c) which is also not sensitive whether coupling exists or not.

Fig. 12(a) and (b) exhibit the response to the cavity formation at $t = 1\,\mu s$ when the Cadmium Selenide material is initially loaded by $\sigma_{23}^0 = 10\,\text{MPa}$ (axial shear) and $D_2^0 = 0.01\,\text{C/m}^2$ in the coupled and uncoupled cases, respectively. In the latter case the stress actually varies in the range $0 \leqslant \sigma_{23}/\sigma_{23}^0 \leqslant 1.1$, but here too it was scaled to confirm with the coupled case of Fig. 12(a). The effect of coupling is clearly noticed. As to the electric displacement distribution D_2/D_2^0, it is identical to the one shown in Fig. 10(c).

The final illustration of the effect of electromechanical coupling is exhibited by Fig. 13(a) and (b) at $t = 1\,\mu s$ in the coupled and uncoupled case, respectively. The initial loading is (as in the previous case): $\sigma_{23}^0 = 10\,\text{MPa}$ (axial shear) but combined with $D_3^0 = 0.01\,\text{C/m}^2$ (i.e., in the poling direction). In addition to the effect of coupling which is illustrated by comparing Fig. 13(a) and (b), it is interesting to observe by comparing Fig. 12(a) with Fig. 13(a) the dramatic effect of the applied electrical displacement direction with respect to the poling direction. The electric displacement distribution D_3/D_3^0 in the present loading case is identical to the one shown in Fig. 11(c).

The formation of a cavity caused by an initially applied transverse shear mechanical loading σ_{12}^0 accompanied by an applied an electrical displacement D_2^0 have been also examined. It turns out that the coupled case is quite identical to the uncoupled one. Thus the electromechanical coupling for such loading is inappreciable.

6. Conclusions

A theory for the simulation of the transient response of piezoelectric composites of periodic microstructure with localized defects has been presented. It forms a continuum theory which couples between an elastodynamic model that has been previously derived and the presently offered method for the treatment of electric field which depends on the mechanical deformations. The defects may represent cracks (one or several interacting cracks), notches, stiff and soft inclusions as well as cavities, which due to their localization, the periodicity of the composite's microstructure is lost. The effects of these defects are represented in the constitutive equations by eigen-electromechanical variables. The derived continuum theory has been verified by comparison with an analytical solution, and application were given for the sudden formation of cracks and cavities under various types of loading. The pronounced effect of electromechanical coupling has been especially illustrated in the sudden formation of cavities. In these applications, the surfaces of the cracks and cavities were assumed to be electrically impermeable, namely, the tractions and normal electric displacement componet there are zero. Permeable solutions how-

ever can be generated by a proper selection of the damage variables.

It is worth mentioning that the present article has been confined to the analysis of the sudden formation of defects but, as has been demonstrated in Aboudi (2013a), it can be extended and applied to obtain the response of piezoelectric composites with localized defects to impulsive electromechanical loadings applied on the boundaries.

Since some piezoelectric materials are brittle, it should be possible to extend the present analysis to the important situation where transverse cracks appear in a cross-ply piezoelectric laminate (where each layer is a piezoelectric material which effectively represents a unidirectional piezoelectric composite. The effective properties can be determined either by a micromechanical analysis or measurements). Under a quasi-static tensile loading along the axial (0-degree) direction, these transverse cracks slightly debond the 0/90 interfaces and might be arrested, but further intense loading generates one or several H-cracks (transverse cracks together with interfacial cracks between the adjacent layers). Finally, the present theory can be also extended to incorporate the magnetic effects in electro-magneto-elastic composites with defects.

Acknowledgment

Appendix: The analysis of two-dimensional wave propagation in piezoelectric composites

In Aboudi (2013a) the analysis of two-dimensional wave propagation in elastic composites with initial stresses and eigen-stresses has been completely described. In the present Appendix the complementary analysis that is required to incorporate the electrical effects is presented. As a result, a continuum model will be established which is capable of analyzing two-dimensional wave propagation in piezoelectric composites. It should be mentioned that although the present derivation is confined to a two-dimensional analysis in which no dependence of the variables on the x_1-direction exists, it is possible to generalize this analysis to a full three dimensional (see Aboudi et al. (2013) for the three dimensional analysis of the elastic case).

As in Aboudi (2013a), the representative cell which is specified by $-2h \leqslant x_2' \leqslant 2h, -2l \leqslant x_3' \leqslant 2l$ is divided into $N_\beta \times N_\gamma$ subcells with $\beta = 1, \ldots, N_\beta, \gamma = 1, \ldots, N_\gamma$, see Fig. 1(c). In addition, $(\bar{x}_2^{(\beta)}, \bar{x}_3^{(\gamma)})$ are local coordinates whose origin is located at the center of the subcell $(\beta\gamma)$, see Fig. 1(d). Just like the mechanical displacement field, the electric potential $\psi^{(\beta\gamma)}$ in subcell $(\beta\gamma)$ is approximated by a second-order expansion in the local coordinates $(\bar{x}_2^{(\beta)}, \bar{x}_3^{(\gamma)})$ as follows (hereafter the 'hat' above the variables has been omitted):

$$\psi^{(\beta\gamma)} = -E_j^{0(\beta\gamma)} x_j + \psi_{(00)}^{(\beta\gamma)} + \bar{x}_2^{(\beta)} \psi_{(10)}^{(\beta\gamma)} + \bar{x}_3^{(\gamma)} \psi_{(01)}^{(\beta\gamma)}$$
$$+ \frac{1}{2}\left(3\bar{x}_2^{(\beta)2} - \frac{h_\beta^2}{4}\right)\psi_{(20)}^{(\beta\gamma)} + \frac{1}{2}\left(3\bar{x}_3^{(\gamma)2} - \frac{l_\gamma^2}{4}\right)\psi_{(02)}^{(\beta\gamma)} \quad (A.1)$$

where $E_j^{0(\beta\gamma)}$ are the induced initial electric field in the subcell caused by the initially applied electric displacements $\boldsymbol{D}^0$ and the time-dependent $\psi_{(00)}^{(\beta\gamma)}$ are the area average potential in the subcell which together with the higher-order time-dependent terms $\psi_{(mn)}^{(\beta\gamma)}; (m+n > 0)$; must be determined.

The electric field components in subcell $(\beta\gamma)$ are obtained from Eq. (5) yielding

$$E_1^{(\beta\gamma)} = E_1^{0(\beta\gamma)}$$
$$E_2^{(\beta\gamma)} = E_2^{0(\beta\gamma)} - \left(\psi_{(10)}^{(\beta\gamma)} + 3\bar{x}_2^{(\beta)} \psi_{(20)}^{(\beta\gamma)}\right) \quad (A.2)$$
$$E_3^{(\beta\gamma)} = E_3^{0(\beta\gamma)} - \left(\psi_{(01)}^{(\beta\gamma)} + 3\bar{x}_3^{(\gamma)} \psi_{(02)}^{(\beta\gamma)}\right)$$

The volume average of Maxwell Eq. (6) yields in conjunction with Eq. (7) and equation (A.4) of Aboudi (2013a) that

$$e_{15}^{(\beta\gamma)} W_{3(20)}^{(\beta\gamma)} + e_{33}^{(\beta\gamma)} W_{3(02)}^{(\beta\gamma)} - \kappa_{11}^{(\beta\gamma)} \psi_{(20)}^{(\beta\gamma)} - \kappa_{33}^{(\beta\gamma)} \psi_{(02)}^{(\beta\gamma)} = 0 \quad (A.3)$$

The surface-average electric potentials $\overset{(2)\pm_{(\beta\gamma)}}{\psi}$ and $\overset{(3)\pm_{(\beta\gamma)}}{\psi}$ are defined by

$$\overset{(2)\pm_{(\beta\gamma)}}{\psi} = \frac{1}{l_\gamma} \int_{-l_\gamma/2}^{l_\gamma/2} \psi^{(\beta\gamma)}\left(\bar{x}_2^{(\beta)} = \pm\frac{h_\beta}{2}\right) d\bar{x}_3^{(\gamma)} \quad (A.4)$$

$$\overset{(3)\pm_{(\beta\gamma)}}{\psi} = \frac{1}{h_\beta} \int_{-h_\beta/2}^{h_\beta/2} \psi^{(\beta\gamma)}\left(\bar{x}_3^{(\gamma)} = \pm\frac{l_\gamma}{2}\right) d\bar{x}_2^{(\beta)} \quad (A.5)$$

Substitution of the electric potential expansion (A.1) in Eq. (A.4) and (A.5) reveals that these surface-average potentials are related to the microvariables $\psi_{(mn)}^{(\beta\gamma)}$ as follows

$$\overset{(2)\pm_{(\beta\gamma)}}{\psi} = \psi_{(00)}^{(\beta\gamma)} \pm \frac{h_\beta}{2} \psi_{(10)}^{(\beta\gamma)} + \frac{h_\beta^2}{4} \psi_{(20)}^{(\beta\gamma)} \quad (A.6)$$

$$\overset{(3)\pm_{(\beta\gamma)}}{\psi} = \psi_{(00)}^{(\beta\gamma)} \pm \frac{l_\gamma}{2} \psi_{(01)}^{(\beta\gamma)} + \frac{l_\gamma^2}{4} \psi_{(02)}^{(\beta\gamma)} \quad (A.7)$$

Manipulation of every pair in these equations results in the following

$$\psi_{(10)}^{(\beta\gamma)} = \frac{1}{h_\beta} \left[\overset{(2)+_{(\beta\gamma)}}{\psi} - \overset{(2)-_{(\beta\gamma)}}{\psi}\right] \quad (A.8)$$

$$\psi_{(01)}^{(\beta\gamma)} = \frac{1}{l_\gamma} \left[\overset{(3)+_{(\beta\gamma)}}{\psi} - \overset{(3)-_{(\beta\gamma)}}{\psi}\right] \quad (A.9)$$

$$\psi_{(20)}^{(\beta\gamma)} = \frac{2}{h_\beta^2} \left[\overset{(2)+_{(\beta\gamma)}}{\psi} + \overset{(2)-_{(\beta\gamma)}}{\psi}\right] - \frac{4}{h_\beta^2} \psi_{(00)}^{(\beta\gamma)} \quad (A.10)$$

$$\psi_{(02)}^{(\beta\gamma)} = \frac{2}{l_\gamma^2} \left[\overset{(3)+_{(\beta\gamma)}}{\psi} + \overset{(3)-_{(\beta\gamma)}}{\psi}\right] - \frac{4}{l_\gamma^2} \psi_{(00)}^{(\beta\gamma)} \quad (A.11)$$

With $W_{3(20)}^{(\beta\gamma)}, W_{3(02)}^{(\beta\gamma)}$ given by Eq. (A.35) and (A.36) of Aboudi (2013a), and $\psi_{(20)}^{(\beta\gamma)}, \psi_{(02)}^{(\beta\gamma)}$ given by (A.10) and (A.11), Eq. (A.3) provides, after some manipulations, the following expression

$$\psi_{(00)}^{(\beta\gamma)} = L_1^{(\beta\gamma)}\left(\overset{(2)+_{(\beta\gamma)}}{u_3} + \overset{(2)-_{(\beta\gamma)}}{u_3}\right) + L_2^{(\beta\gamma)}\left(\overset{(3)+_{(\beta\gamma)}}{u_3} + \overset{(3)-_{(\beta\gamma)}}{u_3}\right)$$
$$+ L_3^{(\beta\gamma)}\left(\overset{(2)+_{(\beta\gamma)}}{\psi} + \overset{(2)-_{(\beta\gamma)}}{\psi}\right) + L_4^{(\beta\gamma)}\left(\overset{(3)+_{(\beta\gamma)}}{\psi} + \overset{(3)-_{(\beta\gamma)}}{\psi}\right)$$
$$+ L_5^{(\beta\gamma)} W_{3(00)}^{(\beta\gamma)} \quad (A.12)$$

where

$$L_1^{(\beta\gamma)} = -\frac{e_{15}^{(\beta\gamma)} l_\gamma^2}{2\left(l_\gamma^2 \kappa_{11}^{(\beta\gamma)} + h_\beta^2 \kappa_{33}^{(\beta\gamma)}\right)}, \quad L_2^{(\beta\gamma)} = -\frac{e_{33}^{(\beta\gamma)} h_\beta^2}{2\left(l_\gamma^2 \kappa_{11}^{(\beta\gamma)} + h_\beta^2 \kappa_{33}^{(\beta\gamma)}\right)},$$

$$L_3^{(\beta\gamma)} = -\frac{\kappa_{11}^{(\beta\gamma)} l_\gamma^2}{2\left(l_\gamma^2 \kappa_{11}^{(\beta\gamma)} + h_\beta^2 \kappa_{33}^{(\beta\gamma)}\right)}, \quad L_4^{(\beta\gamma)} = -\frac{\kappa_{33}^{(\beta\gamma)} h_\beta^2}{2\left(l_\gamma^2 \kappa_{11}^{(\beta\gamma)} + h_\beta^2 \kappa_{33}^{(\beta\gamma)}\right)},$$

$$L_5^{(\beta\gamma)} = \frac{l_\gamma^2 e_{15}^{(\beta\gamma)} + h_\beta^2 e_{33}^{(\beta\gamma)}}{l_\gamma^2 \kappa_{11}^{(\beta\gamma)} + h_\beta^2 \kappa_{33}^{(\beta\gamma)}}$$

$$(A.13)$$

and the variables $W_{3(00)}^{(\beta\gamma)}$ have been already determined by the integration of the mechanical field equations.

The surface-average of the electrical displacements are given by

$$\overset{\pm(\beta\gamma)}{D_2} = \frac{1}{l_\gamma} \int_{-l_\gamma/2}^{l_\gamma/2} D_2^{(\beta\gamma)} \left(\bar{x}_2^{(\beta)} = \pm \frac{h_\beta}{2} \right) d\bar{x}_3^{(\gamma)} \tag{A.14}$$

$$\overset{\pm(\beta\gamma)}{D_3} = \frac{1}{h_\beta} \int_{-h_\beta/2}^{h_\beta/2} D_3^{(\beta\gamma)} \left(\bar{x}_3^{(\gamma)} = \pm \frac{l_\gamma}{2} \right) d\bar{x}_2^{(\beta)} \tag{A.15}$$

By employing Eq. (7), and the strain expressions (A.4) in Aboudi (2013a), we obtain from the above two equations that

$$\overset{\pm(\beta\gamma)}{D_2} = D_2^{0(\beta\gamma)} + e_{15}^{(\beta\gamma)} \left[W_{2(01)}^{(\beta\gamma)} + W_{3(10)}^{(\beta\gamma)} \pm \frac{3h_\beta}{2} W_{3(20)}^{(\beta\gamma)} \right]$$
$$- \kappa_{11}^{(\beta\gamma)} \left[\psi_{(10)}^{(\beta\gamma)} \pm \frac{3h_\beta}{2} \psi_{(20)}^{(\beta\gamma)} \right] - D_2^{e(\beta\gamma)} \tag{A.16}$$

$$\overset{\pm(\beta\gamma)}{D_3} = D_3^{0(\beta\gamma)} + e_{31}^{(\beta\gamma)} W_{2(10)}^{(\beta\gamma)} + e_{33}^{(\beta\gamma)} \left[W_{3(01)}^{(\beta\gamma)} \pm \frac{3l_\gamma}{2} W_{3(02)}^{(\beta\gamma)} \right]$$
$$- \kappa_{33}^{(\beta\gamma)} \left[\psi_{(01)}^{(\beta\gamma)} \pm \frac{3l_\gamma}{2} \psi_{(02)}^{(\beta\gamma)} \right] - D_3^{e(\beta\gamma)} \tag{A.17}$$

where

$$D_2^{0(\beta\gamma)} = 2e_{15}^{(\beta\gamma)} \epsilon_{23}^{0(\beta\gamma)} + \kappa_{11}^{(\beta\gamma)} E_2^{0(\beta\gamma)} \tag{A.18}$$

$$D_3^{0(\beta\gamma)} = e_{31}^{(\beta\gamma)} \left(\epsilon_{11}^{0(\beta\gamma)} + \epsilon_{22}^{0(\beta\gamma)} \right) + e_{33}^{(\beta\gamma)} \epsilon_{33}^{0(\beta\gamma)} + \kappa_{33}^{(\beta\gamma)} E_3^{0(\beta\gamma)} \tag{A.19}$$

being the initial electric displacements induced in the subcells, and $D_2^{e(\beta\gamma)}, D_3^{e(\beta\gamma)}$ are the eigen-electrical displacement portion of $\boldsymbol{Y}^e$ of Eq. (14).

The electric microvariables $\psi_{(mn)}^{(\beta\gamma)}$ in Eq. A.16, A.17 can be expressed in terms of the surface-average potentials. Consequently:

$$\overset{\pm(\beta\gamma)}{D_2} = D_2^{0(\beta\gamma)}$$
$$- \frac{\kappa_{11}^{(\beta\gamma)}}{h_\beta} \left[\overset{(2)+(\beta\gamma)}{\psi} - \overset{(2)-(\beta\gamma)}{\psi} \pm 3 \left(\overset{(2)+(\beta\gamma)}{\psi} + \overset{(2)-(\beta\gamma)}{\psi} - 2\psi_{(00)}^{(\beta\gamma)} \right) \right]$$
$$+ e_{15}^{(\beta\gamma)} \left[W_{2(01)}^{(\beta\gamma)} + W_{3(10)}^{(\beta\gamma)} \pm \frac{3h_\beta}{2} W_{3(20)}^{(\beta\gamma)} \right] - D_2^{e(\beta\gamma)} \tag{A.20}$$

$$\overset{\pm(\beta\gamma)}{D_3} = D_3^{0(\beta\gamma)}$$
$$- \frac{\kappa_{33}^{(\beta\gamma)}}{l_\gamma} \left[\overset{(3)+(\beta\gamma)}{\psi} - \overset{(3)-(\beta\gamma)}{\psi} \pm 3 \left(\overset{(3)+(\beta\gamma)}{\psi} + \overset{(3)-(\beta\gamma)}{\psi} - 2\psi_{(00)}^{(\beta\gamma)} \right) \right]$$
$$+ e_{31}^{(\beta\gamma)} W_{2(10)}^{(\beta\gamma)} + e_{33}^{(\beta\gamma)} \left[W_{3(01)}^{(\beta\gamma)} \pm \frac{3l_\gamma}{2} W_{3(02)}^{(\beta\gamma)} \right] - D_3^{e(\beta\gamma)} \tag{A.21}$$

Where $\psi_{(00)}^{(\beta\gamma)}$ have been already determined in Eq. (A.12).

Eqs. (A.20) and (A.21) can be represented in the following compact form:

$$\left\{ \begin{array}{c} \overset{\pm(\beta\gamma)}{D_2} \\ \overset{\pm(\beta\gamma)}{D_3} \end{array} \right\} = \left\{ \begin{array}{c} D_2^{0(\beta\gamma)} \\ D_3^{0(\beta\gamma)} \end{array} \right\} + [K]^{(\beta\gamma)} \left\{ \begin{array}{c} \overset{(2)\pm(\beta\gamma)}{\psi} \\ \overset{(3)\pm(\beta\gamma)}{\psi} \end{array} \right\} - \left\{ \begin{array}{c} D_2^{e(\beta\gamma)} \\ D_3^{e(\beta\gamma)} \end{array} \right\} + \left\{ \begin{array}{c} M_2^{\pm(\beta\gamma)} \\ M_3^{\pm(\beta\gamma)} \end{array} \right\} \tag{A.22}$$

where $[K]^{(\beta\gamma)}$ is a matrix whose elements involve the electrical properties of the material occupying the subcell $(\beta\gamma)$ and the subcell dimensions, and $M_2^{(\beta\gamma)}, M_3^{(\beta\gamma)}$ consist of a combination of mechanical variables:

$$M_2^{\pm(\beta\gamma)} = e_{15}^{(\beta\gamma)} \left(W_{2(01)}^{(\beta\gamma)} + W_{3(10)}^{(\beta\gamma)} \pm \frac{3h_\beta}{2} W_{2(20)}^{(\beta\gamma)} \right)$$
$$\pm \frac{6}{h_\beta} \kappa_{11}^{(\beta\gamma)} \left[L_1^{(\beta\gamma)} \left(\overset{(2)+(\beta\gamma)}{u_3} + \overset{(2)-(\beta\gamma)}{u_3} \right) + L_2^{(\beta\gamma)} \left(\overset{(3)+(\beta\gamma)}{u_3} + \overset{(3)-(\beta\gamma)}{u_3} \right) + L_5^{(\beta\gamma)} W_{3(00)}^{(\beta\gamma)} \right] \tag{A.23}$$

$$M_3^{\pm(\beta\gamma)} = e_{31}^{(\beta\gamma)} W_{2(10)}^{(\beta\gamma)} + e_{33}^{(\beta\gamma)} \left(W_{3(01)}^{(\beta\gamma)} \pm \frac{3l_\gamma}{2} W_{3(02)}^{(\beta\gamma)} \right)$$
$$\pm \frac{6}{l_\gamma} \kappa_{33}^{(\beta\gamma)} \left[L_1^{(\beta\gamma)} \left(\overset{(2)+(\beta\gamma)}{u_3} + \overset{(2)-(\beta\gamma)}{u_3} \right) + L_2^{(\beta\gamma)} \left(\overset{(3)+(\beta\gamma)}{u_3} + \overset{(3)-(\beta\gamma)}{u_3} \right) + L_5^{(\beta\gamma)} W_{3(00)}^{(\beta\gamma)} \right] \tag{A.24}$$

According to the solution strategy, all the mechanical variables have been already determined at time $t + \Delta t$ by integrating the evolution equation (A.54) in Aboudi (2013a). Hence the only unknowns in Eq. (A.22) are the electric microvariables $\overset{(2)\pm(\beta\gamma)}{\psi}$ and $\overset{(3)\pm(\beta\gamma)}{\psi}$ at time $t + \Delta t$. These are determined from the conditions that the electric potential and normal electric displacements between the subcells must be continuous:

$$\overset{(2)+(\beta\gamma)}{\psi} = \overset{(2)-(\beta+1,\gamma)}{\psi}, \quad \beta = 1, \ldots, N_\beta - 1, \ \gamma = 1, \ldots, N_\gamma \tag{A.25}$$

$$\overset{(3)+(\beta\gamma)}{\psi} = \overset{(3)-(\beta,\gamma+1)}{\psi}, \quad \beta = 1, \ldots, N_\beta, \ \gamma = 1, \ldots, N_\gamma - 1 \tag{A.26}$$

$$\overset{(\beta\gamma)}{D_2} = \overset{(\beta+1,\gamma)}{D_2}, \quad \beta = 1, \ldots, N_\beta - 1, \ \gamma = 1, \ldots, N_\gamma \tag{A.27}$$

$$\overset{(\beta\gamma)}{D_3} = \overset{(\beta,\gamma+1)}{D_3}, \quad \beta = 1, \ldots, N_\beta, \ \gamma = 1, \ldots, N_\gamma - 1 \tag{A.28}$$

These together with the continuity conditions between the cells in the transform domain yield a system of $8N_\beta N_\gamma$ algebraic equations (in the complex plane) with the same number of unknowns to be solved. This system can be formally represented as:

$$\boldsymbol{T}\boldsymbol{X}(t + \Delta t) = \boldsymbol{N}(t + \Delta t) \tag{A.29}$$

where $\boldsymbol{T}$ is time-independent matrix which depends on the electrical properties of the constituents and subcells geometry, $\boldsymbol{X}$ a time-dependent vector consisting of the electric potential microvariables, and $\boldsymbol{N}$ is time-dependent vector that involve the mechanical variables and eigen-electrical displacements at time $t + \Delta t$ as well as the electrical applied loadings. The solution of this system of equations enables the determination of all electrical field variables.

References

Aboudi, J., 1987. Transient waves in composite materials. Wave Motion 9, 141–156.

Aboudi, J., 2001. Micromechanical analysis of fully coupled electro-magneto-thermo-elastic multiphase composites. Smart Mater. Struct. 10, 867–877.

Aboudi, J., 2013a. Dynamic field distributions generated by localized effects in periodically layered composites. Int. J. Solids Struct. 50, 456–471.

Aboudi, J., 2013b. Field distributions in cracked periodically layered electro-magneto-thermo-elastic composites. J. Intell. Mater. Syst. Struct. 24, 381–398.

Aboudi, J., Arnold, S.M., Bednarcyk, B.A., 2013. Micromechanics of Composite Materials: A Generalized Multiscale Analysis Approach. Elsevier, Oxford, UK.

Achenbach, J.D., 1973. Wave Propagation in Elastic Solids. North Holland Publishing Co., Amsterdam.

Achenbach, J.D., 2000. Quantitative nondestructive evaluation. Int. J. Solids Struct. 37, 13–27.

Auld, B.A., 1973. Acoustic Fields and Waves in Solids, vol. 1. Wiley, New York.

Baker, B.R., 1962. Dynamic stresses created by a moving crack. J. Appl. Mech. 29, 449–458.

Chee, C., Tong, L., Steven, G.P., 1998. A review on the modelling of piezoelectric sensors and actuators incorporated in intelligent structures. J. Intell. Mater. Syst. Struct. 9, 3–19.

Chen, J., Pan, E., Chen, H., 2007. Wave propagation in magneto-electro-elastic multilayered plates. Int. J. Solids Struct. 44, 1073–1085.

Du, J., Xian, K., Wang, J., 2009. SH surface acoustic wave propagation in a cylindrically layered piezomagnetic/piezoelectric structure. Ultrasonics 49, 131–138.

Freund, L.B., 1990. Dynamic Fracture Mechanics. Cambridge University Press, Cambridge, UK.

Ju, J.W., 1990. Isotropic and anisotropic damage variables in continuum damage mechanics. J. Eng. Mech. 116, 2764–2770.

Li, X.-F., 2001. Transient response of a piezoelectric material with a semi-infinite mode-III crack under impact loads. Int. J. Fract. 111, 119–130.

Miklowitz, J., 1960. Plane-stress unloading waves emanating from a suddenly punched hole in a stretched elastic hole. J. Appl. Mech. 27, 165–171.

Nayfeh, A.H., Waseem, F., Abdelrahman, W., 1999a. Approximate model for wave propagation in piezoelectric material. I. Laminated composites. J. Appl. Phys. 85, 2337–2346.

Nayfeh, A.H., Dong, J.J., Waseem, F., 1999b. Approximate model for wave propagation in piezoelectric material. II. Fibrous composites. J. Appl. Phys. 85, 2347–2354.

Pak, Y.E., 1990. Crack estension force in a piezoelectric material. J. Appl. Mech. 57, 647–653.

Pak, Y.E., 1992. Circular inclusion problem in antiplane piezoelectricity. Int. J. Solids Struct. 19, 2403–2419.

Pang, Y., Liu, J., Wang, Y., Fang, D., 2008. Wave propagation in piezoelectric/piezomagnetic layered periodic composites. Acta Mech. Solida Sinica 21, 483–490.

Parton, V.Z., Kudryavtsev, B.A., 1988. Electromagnetoelasticity: Piezoelectrics and Electrically Conductive Solids. Gordon Breach, New York.

Qin, Q.-H., 2001. Fracture Mechanics of Piezoelectric Material. WIT press, Southampton.

Rao, S.S., Sunar, M., 1994. Piezoelectricity and its use in disturbance sensing and control of flexible structures: a survey. Appl. Mech. Rev. 47, 113–123.

Rizzo, P., Lanza di Scalea, F., 2007. Wavelet-based unsupervised and supervised learning algorithms for ultrasonic structural monitoring of waveguides. In: Reece, P. (Ed.), Progress in Smart Materials and Structures. Nova Science Publishers, New York.

Rose, J.L., 1999. Ultrasonic Waves in Solid Media. Cambridge University Press, Cambridge, UK.

Ryvkin, M., Nuller, B., 1997. Solution of quasi-periodic fracture problems by the representative cell method. Comput. Mech. 20, 145–149.

Saravanos, D.A., Hopkins, D.A., 1996. Effects of delaminations on the damped dynamic characteristics of composite laminates: analysis and experiments. J. Sound Vib. 192, 977–993.

Saravanos, D.A., Birman, V., Hopkins, D.A., 1994. Detection of delamination in composite beams using piezoelectric sensors. NASA/TM 106611.

Sosa, H., 1991. Plane problems in piezoelectric media with defects. Int. J. Solids Struct. 28, 491–505.

Talreja, R., Singh, C.V., 2012. Damage and Failure of Composite Materials. Cambridge University Press, Cambridge, UK.

Tan, P., Tong, L., 2007. Experimental and analytical identification of a delamination using isolated PZT sensor and actuator patches. J. Compos. Mater. 41, 477–492.

Wang, R., Qingkai, H., Pan, E., 2011. Transient response of a bi-layered multiferroic composite plate. Acta Mech. Solida Sinica 24, 83–91.

Winzer, S.R., Shankar, N., Ritter, A., 1989. Designing corfired multilayer electrostrictive actuators for reliability. J. Am. Ceram. Soc. 72, 2246–2257.